Implied Stopping Rules for American Basket Options from Markovian Projection

CHRISTIAN BAYER, JUHO HÄPPÖLÄ, AND RAUL TEMPONE

ABSTRACT. This work addresses the problem of pricing American basket options in a multivariate setting, which includes among others, the Bachelier and the Black-Scholes models. In high dimensions, nonlinear partial differential equation methods for solving the problem become prohibitively costly due to the curse of dimensionality. Instead, this work proposes to use a stopping rule that depends on the dynamics of a low-dimensional Markovian projection of the given basket of assets. It is shown that the ability to approximate the original value function by a lower-dimensional approximation is a feature of the dynamics of the system and is unaffected by the path-dependent nature of the American basket option. Assuming that we know the density of the forward process and using the Laplace approximation, we first efficiently evaluate the diffusion coefficient corresponding to the low-dimensional Markovian projection of the basket. Then, we approximate the optimal early-exercise boundary of the option by solving a Hamilton-Jacobi-Bellman partial differential equation in the projected, low-dimensional space. The resulting near-optimal early-exercise boundary is used to produce an exercise strategy for the high-dimensional option, thereby providing a lower bound for the price of the American basket option. A corresponding upper bound is also provided. These bounds allow to assess the accuracy of the proposed pricing method. Indeed, our approximate early-exercise strategy provides a straightforward lower bound for the American basket option price. Following a duality argument due to Rogers, we derive a corresponding upper bound solving only the low-dimensional optimal control problem. Numerically, we show the feasibility of the method using baskets with dimensions up to fifty. In these examples, the resulting option price relative errors are only of the order of few percent.

1. INTRODUCTION

This work addresses the problem of pricing American basket options in a multivariate setting. Our approach relies on a stopping rule that depends on the dynamics of a low-dimensional Markovian projection of the given basket of assets.

Pricing path-dependent options is a notoriously difficult problem. Even for relatively simple cases, such as the Black-Scholes model or the Bachelier model, in which an analytic expression of the risk-neutral expected payoff at a terminal time, T, can be found, prices of path-dependent options, such as American options, must typically be solved for numerically. This difficulty is aggravated in high dimensions, where convergence rates of well-known numerical methods deteriorate exponentially as the number of dimensions increases. However, there is a plethora of American options being offered in the markets, in publicly traded markets or over-the-counter (OTC). Perhaps the best-known example is that of options written the S&P-100 index quoted on the Chicago Board Options Exchange (CBOE). In addition, the wide variety of exchange traded funds (ETF) tracking indices have American options written on them publicly quoted on CBOE. These funds include

many prominent indices such as Euro Stoxx 50 and the Dow Jones Industrial average, as well as many regional indices.

The two most widely used approaches to pricing path-dependent options, binomial tree methods and partial differential equation (PDE) methods, both suffer from the so-called curse of dimensionality. In the case of the probability trees or lattices, the size of the probabilistic trees, even in the case of recombining trees, already becomes prohibitively large in moderate dimensions. The other popular method requires solving the Black-Scholes equation using finite difference (FD) or finite element (FEM) methods. Both methods involve discrete differential operators whose size also scales exponentially in the number of dimensions.

In Monte Carlo simulation, the rate of convergence of weak approximations does not explicitly depend on the number of dimensions. With early-exercise options like American ones, however, Monte Carlo methods become more complicated. Although well suited for forward-propagation of uncertainties in a wide range of models, traditional Monte Carlo methods do not offer a straightforward way to construct an exercise strategy. Such a strategy typically needs to be obtained through backward induction. Because the price of an American option is based on assuming optimal execution of the option, any solution scheme needs to produce the optimal stopping strategy as a by-product of the pricing method. Many methods have been developed to produce a near-optimal execution strategy. Broadie and Glasserman (1997) introduced a pair of schemes that evaluate upper and lower bounds of the prices of American options. Longstaff and Schwartz (2001) used least-squares regression in conjunction with Monte Carlo simulation to evaluate the price of American options. Their popular method has been widely implemented in various pricing engines, for example in the QuantLib library by Ametrano and Ballabio (2003).

In the least-squares Monte Carlo methodology, the value of holding an option is weighed against the cash flow captured by exercising the option. The intrinsic value of an option is, of course, known. However, the holding price is the discounted expectation of possible future outcomes. This expectation is estimated based on a Monte Carlo sample by regressing the holding price of the option to a few of decision variables or basis functions. Naturally, the choice of the appropriate basis functions has a crucial effect on the quality of the outcome, and also the number of basis functions should be much smaller than the size of the Monte Carlo sample to avoid overfitting(Glasserman *et al.*, 2004; Zanger, 2013, 2016). For work on the reduction of the computational complexity in the regression methods, we refer the reader to Belomestny *et al.* (2013, 2015).

Another method to approximate option prices in high dimensions is the optimal quantizer approach of Bally *et al.* (2005). In this method the diffusion process is projected to a finite mesh. This mesh is chosen optimally to minimize projection error, the conditional expectation describing the holding price is then evaluated at each of the mesh points. The quantization tree approach gives accurate approximations of the option price in moderate dimension. Here, we present methods for selected parametrisations of the Black-Scholes model over twice the dimension presented in (Bally *et al.*, 2005) For work with rather large number of dimensions, we refer the reader to the stratified state aggregation along payoff (SSAP) method of (Barraquand and Martineau, 1995). In the SSAP method, one solves for an exercise strategy through stratifying possible values of the intrinsic value of the option.

Here, we propose and analyze a novel method for pricing American options written on a basket of assets. Like the SSAP, the pricing method in this work relies on using the intrinsic value, or the value of the underlying asset as a state variable. On the other hand, our method is based on the Markovian projection of the underlying asset, does not rely on

the use of basis functions and provides upper and lower bounds for the option price. These bounds are useful to assess the accuracy of our methodology.

In this exploratory work, we computationally study the feasibility of using stopping rules based on a simplified surrogate process in pricing American options written on a basket of assets. The method offers an efficient approximation to pricing and hedging American options written on an index, or a security tracking such index. Instead of the full-dimensional process, we use a lower-dimensional process obtained through Markovian projection. Even though the evolution of the multiple assets involved in a given basket is usually assumed Markovian, the SDE describing the evolution of a linear combination or a basket of assets, is rarely Markovian in the basket value. We address this issue by means of Markovian projection, which provides a low-dimensional Markovian SDE that is suited to dynamic programming (DP) methods that solve the relevant Hamilton-Jacobi-Bellman (HJB) equation. Markovian projection techniques have been previously applied to a range of financial applications, see, for example, (Piterbarg, 2003, 2005; Djehiche and Löfdahl, 2014).

Outline. The remainder of this work is organized as follows. In Section 2, we describe the Markovian projection in the context of projecting high-dimensional SDEs into lower dimensions. We show how the low-dimensional HJB equation gives rise to a stopping rule that in general is sub-optimal but provides a lower bound for the American option price. Using a duality approach from Rogers (2002), we give an upper bound for the option price using the solution of the low-dimensional HJB equation. We show that in the Bachelier model, the lower and upper bounds coincide and provide an exact option valuation. We prove how the question of whether the cost-to-go function of an American option can be approximated using a low-dimensional approximation reduces to the corresponding question of European options, which are simpler to analyze. It is known that the Bachelier model is a close approximation to the Black-Scholes model in the realm of European option pricing (Schachermayer and Teichmann, 2008). We motivate that this approximation has a beneficial effect when pricing American basket options with our methodology since our method is exact for the Bachelier model. In Section 3, we detail the numerical implementation of the ideas developed in the preceding section and experiment with multivariate Bachelier and Black-Scholes models. Reporting results of numerical experiments, we verify the accuracy of our method with the Bachelier model and give supporting results to justify the use of our method in cases where neither the European or American option prices can be precisely represented using a low-dimensional approximation. Using the Black-Scholes model as an example, we show that the approximation error of our method is few per cent, comparable to the bid-ask spread of even the more liquid openly traded options and well within the spread of more illiquid index options or options quoted on an ETF. Finally, we offer concluding remarks in Section 4.

2. Markovian projections and implied stopping times

In this section, we revisit the essential equations that describe risk-neutral option pricing of American options in a multivariate setting. We present in Section 2.1 how these equations have corresponding low-dimensional projections that can be obtained using the Markovian projection. In Section 2.2, we show how the projected PDEs give rise to lower and upper bounds for the solution of the original high-dimensional pricing problem.

Following the introduction of the relevant bounds, we discuss in Section 2.3 classes of models that are of particular interest in reduced-dimension evaluation. First, we recall in

Lemma 2.7 how the Gaussian Bachelier model has the feature that the Markovian projection produces a one-dimensional SDE whose solution coincides in law with the underlying high-dimensional portfolio. We also show in Corollary 2.8 how this one-dimensional approximation property is preserved if the Bachelier model is generalized through the appropriate introduction of a stochastic clock. Secondly, we provide auxiliary results to characterize some Itô SDEs that have this exact reduced dimension structure that our proposed method exploits. Among these ancillary results, we have Lemma 2.12, which we use to reduce the discussion of dimension reduction of American options into the problem of analyzing low-dimensional approximations of the corresponding European option. Furthermore, we give a motivation for using the Markovian projection even for models that do not have the exact reduced dimension property.

2.1. **Markovian projections and approximate stopping times.** Assume that the time evolution of the asset prices in the basket is given by a stochastic process in $\mathbb{R}^d$, $X(t, \omega)$, that is the unique strong solution to an Itô SDE,

$$
\begin{aligned}
\mathrm{d}X(t) &= a(t, X(t)) \,\mathrm{d}t + \mathbf{b}(t, X(t)) \,\mathrm{d}W(t), \ 0 < t < T, \\
X(0) &= x_0,
\end{aligned}
\tag{1}
$$

which is driven by a k-dimensional Wiener process with independent components, W. We work under the risk-neutral measure and due to a no arbitrage assumption, the drift in (1) is a linear function,

$$
a(t, x) = rx,
\tag{2}
$$

where $r \in \mathbb{R}$ is the short rate. Most of the discussion can also be generalized with minimal modifications to a time-dependent, stochastic, short rate when the short rate process is independent of the dynamics of the underlying assets, see Remark 2.11. For $1 \le i \le d$ and $1 \le j \le k$ the diffusion coefficients, b_{ij}, are at least second order differentiable functions and such that the pdf of $X(t)$ exists for $0 < t \le T$ and is a univariate, smooth function, cf. Assumption 3.1. Furthermore, we denote the canonical filtration generated by $X(t)$ as $\mathcal{F}_t = \sigma\{X(q) : 0 \le q \le t\}$.

In the numerical examples in the subsequent section, we directly deal with the models of Bachelier (Sullivan and Weithers, 1991) and Black-Scholes (Black and Scholes, 1973), acknowledging possible extensions to the constant elasticity of variance (CEV) model (see Cox (1975)) that can in a certain sense be understood as a compromise between the Bachelier and Black-Scholes models. Many other extensions are also possible, and we discuss some of them in Section 2.3. Note the time-homogeneous structure of the examined models and recognize possible extensions to time-inhomogeneous models, for instance by using temporal reparametrization.

Furthermore, we assume for simplicity that the underlying pays no dividends. This work focuses extensively on models of Bachelier and Black-Scholes type. They are defined by their respective volatilities, namely

$$
\mathbf{b}_{\text{Bachelier}}(t, x) = \Sigma,
\tag{3}
$$

$$
b_{\text{Black-Scholes},ij}(t, x) = x_i \Sigma_{ij}.
\tag{4}
$$

with $\Sigma \in \mathbb{R}^{d \times k}$ in both models.

We focus on a portfolio of assets, S_1, given by weights $\mathbf{P}_1$,

$$
S_1(t) = \mathbf{P}_1 X(t),
\tag{5}
$$

as the underlying security, for $\mathbf{P}_1 \in \mathbb{R}^{1 \times d}$, with non-zero elements, possibly some but not all negative. We seek to price options with the payoff functional $g : \mathbb{R} \to \mathbb{R}$. Arguably, the most interesting example is that of the put option, $g(s) = (K - s)^+$ for some $K \in \mathbb{R}$.

The price of the European option written on the portfolio $\mathbf{P}_1$ with expiry at T is given by

(6)
$$u_E(t, \boldsymbol{x}) = \mathrm{E}\left[\exp\left(-r\left(T - t\right)\right) g\left(\mathbf{P}_1 X(T)\right) | X(t) = \boldsymbol{x}\right].$$

In contrast, when pricing American options, we seek to solve for

(7)
$$u_A(t, \boldsymbol{x}) = \sup_{\tau \in \mathcal{T}_t} \mathrm{E}\left[\exp\left(-r\left(\tau - t\right)\right) g\left(\mathbf{P}_1 X(\tau)\right) | X(t) = \boldsymbol{x}\right],$$
$$\mathcal{T}_q = \{\tau : \Omega \to [q, T] | \{\tau \leq t\} \in \mathcal{F}_t, \ \forall t \in [q, T]\}.$$

The European option price u_E given by (6) also satisfies the Black-Scholes equation in $(t, \boldsymbol{x}) \in [0, T] \times D$,

(8)
$$-\partial_t u_E(t, \boldsymbol{x}) = -r u_E(t, \boldsymbol{x}) + \sum_i \boldsymbol{a}_i(t, \boldsymbol{x}) \partial_{x_i} u_E(t, \boldsymbol{x}) + \frac{1}{2} \sum_{ij} \left(\mathbf{bb}^\mathrm{T}\right)_{ij}(t, \boldsymbol{x}) \partial^2_{x_i x_j} u_E(t, \boldsymbol{x})$$
$$u_E(T, \cdot) = g\left(\mathbf{P}_1 \cdot\right),$$

with the appropriate domain $D \subset \mathbb{R}^d$. For example, in the Black-Scholes model, we have $D = D^d_{BS} = \mathbb{R}^d_+$ with the appropriate Dirichlet boundary condition at hyperplanes at which one or more components of $X(t)$ are zero. The boundary value is given by a lower-dimensional version of (8). Defining the second order linear differential operator

$$\left(\mathcal{L}v\right)(t, \boldsymbol{x}) = \left(-r + \sum_i \boldsymbol{a}_i \partial_{x_i} + \frac{1}{2} \sum_{ij} \left(\mathbf{bb}^\mathrm{T}\right)_{ij} \partial^2_{x_i x_j}\right)(t, \boldsymbol{x}) \, v(t, \boldsymbol{x}),$$

we can write the corresponding non-linear HJB equation. Following the presentation of Achdou and Pironneau (2005, equation (6.2)), the American option price, u_A, satisfies

$$\left(\mathcal{L}u_A + \partial_t u_A\right)(t, \boldsymbol{x}) \leq 0, \qquad\qquad (t, \boldsymbol{x}) \in [0, T] \times D,$$
$$u_A(t, \boldsymbol{x}) \geq g\left(\mathbf{P}_1 \boldsymbol{x}\right), \qquad\qquad (t, \boldsymbol{x}) \in [0, T] \times D,$$
$$\left(\left(\mathcal{L}u_A + \partial_t u_A\right)(t, \boldsymbol{x})\right)\left(u_A(t, \boldsymbol{x}) - g\left(\mathbf{P}_1 \boldsymbol{x}\right)\right) = 0, \qquad\qquad (t, \boldsymbol{x}) \in [0, T] \times D.$$

Introducing the Hamiltonian,

(9)
$$\left(\mathcal{H}u_A\right)(t, \boldsymbol{x}) = \left(\mathcal{L}u_A\right)(t, \boldsymbol{x}) \, \mathbf{1}_{\max\left(\left(\mathcal{L}u_A\right)(t, \boldsymbol{x}), \ u_A(t, \boldsymbol{x}) - g(\mathbf{P}_1 \boldsymbol{x})\right) > 0},$$

we write the HJB equation for u_A shortly as

(10)
$$-\partial_t u_A(t, \boldsymbol{x}) = \left(\mathcal{H}u_A\right)(t, \boldsymbol{x}), \ (t, \boldsymbol{x}) \in [0, T] \times D,$$
$$u_A(t, \cdot) = g\left(\mathbf{P}_1 \cdot\right).$$

For the Bachelier model, D is unbounded. For the Black-Scholes model, one or more components of $X(t)$ vanish at the boundary ∂D. Since both the drift (2) and the volatility (4) are linear in their arguments, the drift and the volatility vanish at the boundary. Resulting boundary value is thus given by a lower-dimensional variant of equation (10) where one or more of the components of $X(t)$ are fixed to zero.

Instead of trying to solve (10) directly, we first turn our attention to a low-dimensional approximation of the portfolio process S_1 introduced in (5). This approximation is the

Markovian projection of S_1 (Gyöngy, 1986; Piterbarg, 2006). Indeed, we approximate the non-Markovian evolution of S_1 by the following surrogate process,

(11)
$$\mathrm{d}\overline{S}^{(x_0)}(t) = \overline{a}^{(x_0)}\left(t, \overline{S}^{(x_0)}(t)\right)\mathrm{d}t + \overline{b}^{(x_0)}\left(t, \overline{S}^{(x_0)}(t)\right)\mathrm{d}W(t), \ t \in [0, T],$$
$$\overline{S}^{(x_0)}(0) = \mathbf{P}_1 x_0,$$

The drift and volatility coefficients in (11) are evaluated through conditional expectations, namely

(12)
$$\overline{a}^{(x_0)}(t, s) = \mathrm{E}\left[\mathbf{P}_1 a\left(t, X(t)\right) | \mathbf{P}_1 X(t) = s, \ X(0) = x_0\right],$$

(13)
$$\left(\overline{b}^{(x_0)}\right)^2(t, s) = \mathrm{E}\left[\left(\mathbf{P}_1 \mathbf{b}\mathbf{b}^{\mathrm{T}}\mathbf{P}_1^{\mathrm{T}}\right)(t, X(t)) | \mathbf{P}_1 X(t) = s, \ X(0) = x_0\right].$$

The Markovian projection (11) generates its canonical filtration, $\overline{\mathcal{F}}_t = \sigma\left\{\overline{S}^{(x_0)}(q) : 0 \leq q \leq t\right\}$.

Observe that the surrogate process, $\overline{S}^{(x_0)}(t)$ in (11), has, due to the proper selection of the drift and volatility functions and the appropriate initial value, the same marginal density as $S(t) = \mathbf{P}_1 X(t)$ for all $t \in [0, T]$ (Gyöngy, 1986). For any given payoff function g that yields a finite price in (6), this implies the identity

(14)
$$\mathrm{E}\left[\exp\left(-rT\right) g\left(\mathbf{P}_1 X(T)\right) | X(0) = x_0\right] = \mathrm{E}\left[\exp\left(-rT\right) g\left(\overline{S}^{(x_0)}(T)\right) | \overline{S}^{(x_0)}(0) = \mathbf{P}_1 x_0\right],$$

which means that we can price European options on the basket using only our knowledge of the Markovian process $\overline{S}^{(x_0)}$.

Assuming that we know the dynamics (11), we can evaluate the right-hand side of equation (14) using the Feynman-Kac Formula. By denoting

(15)
$$\overline{u}_E(t, s) = \mathrm{E}\left[\exp\left(-r(T - t)\right) g\left(\overline{S}^{(x_0)}(t)\right) | \overline{S}^{(x_0)}(t) = s\right],$$

we have that $\overline{u}_E$ solves a corresponding linear backward PDE in one space dimension only,

(16)
$$-\partial_t \overline{u}_E(t, s) = \underbrace{-r\overline{u}_E(t, s) + \overline{a}^{(x_0)}(t, s)\partial_s \overline{u}_E(t, s) + \frac{\left(\overline{b}^{(x_0)}\right)^2(t, s)}{2}\partial_{ss}^2 \overline{u}_E(t, s)}_{\equiv \left(\overline{\mathcal{L}}\overline{u}_E\right)(t,s)}, \ t \in [0, T], \ s \in \overline{D},$$

$$\overline{u}_E(T, \cdot) = g(\cdot).$$

Remark 2.1 (Interpretation of projected PDEs). We have defined the projected PDE (16) that is of Black-Scholes type. Furthermore, the coefficients $\overline{a}^{(x_0)}$ and $\overline{b}^{(x_0)}$ of the equation are constructed through conditioning to the initial value of the SDE (1). Here, we use the the PDE (16) as a mathematical construct to evaluate the expectation (14). We do not interpret the solution of equation (16), or its extensions defined in the remainder of this work as tradeable option prices.

Note that the procedure above can be generalized to cases where the Markovian projection is carried out onto a space of dimension $\overline{d} > 1$. This is done simply by introducing additional portfolios and their weights, $\mathbf{P}^{\mathrm{T}} = [\mathbf{P}_1^{\mathrm{T}}, \mathbf{P}_2^{\mathrm{T}}, \mathbf{P}_3^{\mathrm{T}}, \ldots, \mathbf{P}_{\overline{d}}^{\mathrm{T}}]$, and defining the multidimensional dynamics for $\overline{S}^{(x_0)}$ via the projected volatility coefficients as

(17)
$$\left(\mathbf{b}\mathbf{b}^{\mathrm{T}}\right)_{ij}^{(x_0)}(t, s) = \mathrm{E}\left[\left(\mathbf{P}_i^{\mathrm{T}}\mathbf{b}\mathbf{b}^{\mathrm{T}}\mathbf{P}_j\right)(t, X(t)) | \mathbf{P}X(t) = s, \ X(0) = x_0\right], \ 1 \leq i, j \leq \overline{d}.$$

Summing up, as long as we can efficiently evaluate the coefficients in the SDE (11), it is possible to solve the low-dimensional equation (16) instead of equation (8) that suffers from the curse of dimensionality. Obviously, the efficient evaluation of the coefficients in the SDE of $\overline{S}^{(x_0)}$ via conditional expectation as in (13) is in principle a daunting task. Section 3.1.1 proposes an efficient approximation to carry out this evaluation.

Remark 2.2 (Computational domains and boundary conditions). Instead of using the full unbounded domain of the PDE (16) in the numerical part of this work, we use a modified, computational domain, on which we impose an artificial boundary condition as follows.

First, note that the appropriate domain, D, for (8) depends on the model of choice. For the d-dimensional Black-Scholes model, we have $D = D_{\text{Black-Scholes}}^d = \mathbb{R}_+^d$ and correspondingly for the Bachelier model, $D = D_{\text{Bachelier}}^d = \mathbb{R}^d$. When numerically solving the full, d-dimensional equation (8), one often truncates the domain into a compact one and imposes artificial boundary conditions on the boundary of the localized computational domain. Here, we also truncate the projected domain, $\overline{D}$, into a localized computational domain. At the boundary of the computational domain, we impose the artificial boundary condition $\bar{u}(t, s) = g(s)$. In addition to the truncation, we note that the coefficients of the equation (16) are defined only for regions where the density ϕ of process $\mathbf{P}_1 X(t)$ has support. We extend artificially the domain of (16) to the rectangle $[0, T] \times [s_{\min}, s_{\max}]$ by extrapolating the relevant coefficients $\overline{a}^{(x_0)}$ and $\left(\overline{b}^{(x_0)}\right)^2$. For $\left(\overline{b}^{(x_0)}\right)^2$ we also set a lower bound to guarantee numerical stability and well-posedness.

In all our numerical examples, we make sure that our truncated and extrapolated computational domain is sufficiently large to make the corresponding domain truncation error negligible. For more in-depth discussions on this matter, we refer the reader to (Kangro and Nicolaides, 2000; Choi and Marcozzi, 2001; Matache *et al.*, 2004; Hilber *et al.*, 2004).

Furthermore, to maintain brevity of notation, we will refrain from writing explicitly the artificial boundary conditions. All relevant PDEs in this work are understood to be numerically solved using Dirichlet boundary conditions implied by the intrinsic value of the option.

Just as the Black-Scholes equation, (8) has a corresponding HJB equation (10), we may use the corresponding HJB to the projected Black-Scholes equation (16). The resulting HJB equation describes the cost-to-go function $\bar{u}_A$ of an American option written on the portfolio that has the projected dynamics of equation (11):

(18)
$$-\partial_t \bar{u}_A (t, s) = \left(\overline{\mathcal{L}} \bar{u}_A\right)(t, s) \, \mathbf{1}_{\max\left(\left(\overline{\mathcal{L}} \bar{u}_A\right)(t,s), \, \bar{u}_A(t,s) - g(s)\right) > 0} = \left(\overline{\mathcal{H}} \bar{u}_A\right)(t, s) \quad (t, s) \in [0, T] \times \overline{D},$$
$$\bar{u}_A (T, \cdot) = g(\cdot).$$

However, for American option prices, there is no identity corresponding to equality (14). As a result, the magnitude of the difference $|\bar{u}_A (0, \mathbf{P}_1 x_0) - u_A (0, x_0)|$ may not necessarily be small. Also, the boundary conditions of equation (18) are subject to the same ambiguity as the ones of equation (16) discussed in Remark 2.2. The main focus of this work is to address these issues and to estimate the difference between the computed value of $\bar{u}_A$ and the sought u_A, which is assumed beyond our reach being too costly to compute.

We note in passing that the processes X and $\overline{S}^{(x_0)}$ live in different probability spaces. Likewise, the stopping times corresponding to the full-dimensional and projected SDE are adapted to $\mathcal{F}_t$ and $\overline{\mathcal{F}}_t$, respectively.

2.2. **Implied stopping time and price bounds.** Above we have laid out the question of the feasibility of using the projected dynamics $\overline{S}^{(x_0)}$ in pricing American options, we now show below in Section 2.2.1 how the solution of the projected problem $\overline{u}_A$ gives rise to an exercise strategy that is sub-optimal. This sub-optimal exercise strategy gives a lower bound for the option price. We complement this lower bound with a corresponding upper bound in Section 2.2.2.

2.2.1. *Lower bound.* In the full American option pricing problem (7), the optimal stopping time, $\tau^* \in \mathcal{T}_0$, such that

$$u_A(0, x_0) = \mathrm{E}\left[\exp\left(-r\tau^*\right) g\left(\mathbf{P}_1 X\left(\tau^*\right)\right) | X(0) = x_0\right],$$

is given by

(19) $$\tau^* = \inf\left\{t \in [0, T] : u_A(t, X(t)) = g\left(\mathbf{P}_1 X(t)\right)\right\}.$$

Any stopping time $\tau \in \mathcal{T}_0$ gives a lower bound for the option price. We do not have access to the full cost-to-go function, u_A, and hence a natural replacement is given by the projected cost-to-go function $\overline{u}_A$. Indeed, the projected cost-to-go function $\overline{u}_A$ gives rise to two hitting times:

$$\overline{\tau}^* \equiv \inf\left\{t \in [0, T] : \overline{u}_A\left(t, \overline{S}^{(x_0)}(t)\right) = g\left(\overline{S}^{(x_0)}(t)\right)\right\},$$

where the dynamics of $\overline{S}$ is given by (11) and

(20) $$\overline{\tau}^\dagger \equiv \inf\left\{t \in [0, T] : \overline{u}_A(t, \mathbf{P}_1 X(t)) = g\left(\mathbf{P}_1 X(t)\right)\right\}.$$

We note that due to the terminal condition on $\overline{u}_A$ in equation (18) all hitting times are bounded by T.

We conclude the discussion on the lower bound of the option value by stating the lower bound implied by the hitting time $\overline{\tau}^\dagger \in \mathcal{T}_0$,

(21) $$u_A(0, x_0) \geq \mathrm{E}\left[\exp\left(-r\overline{\tau}^\dagger\right) g\left(\mathbf{P}_1 X\left(\overline{\tau}^\dagger\right)\right) | X(0) = x_0\right].$$

We emphasize that we have not made a comparison between $u_A(0, x_0)$ and $\overline{u}_A(0, \mathbf{P}_1 x_0)$.

Remark 2.3 (On least-squares Monte Carlo). The approach we have adopted shares some similarities with the least-squares Monte Carlo approach. However, there are key differences: In the least-squares Monte Carlo method, the stopping time can be understood as a hitting time into a region where the holding value of the option, as estimated through regression to a set of basis functions, is exceeded by the early exercise price. The hitting time (20) is likewise defined as a comparison between the estimated cost-to-go function, $\overline{u}_A$, and the early exercise price. However, the estimated cost-to-go function, $\overline{u}_A$, does not depend on a choice of basis functions, only on the direction of the projection. On the other hand, $\overline{u}_A$ is constructed using the Markovian projection $\overline{S}^{(x_0)}$ instead of the true forward model X.

2.2.2. *Upper bound.* To assess the accuracy of approximating the process with a low-dimensional Markovian projection, we want to devise a corresponding upper bound. For this, we use the dual representation due to Rogers (2002).

The dual representation of the pricing problem is as follows. The price of the American option is given by:

(22) $$u_A(0, x_0) = \inf_{R \in H_0^1} \mathrm{E}\left[\sup_{0 \leq t \leq T}\left(\tilde{Z}(t) - R(t)\right) | X(0) = x_0\right],$$

where H_0^1 denotes the space of all integrable martingales R, $t \in [0, T]$ such that for $R \in H_0^1$

$$\sup_{0 \leq t \leq T} |R(t)| \in L^1,$$
$$R(0) = 0.$$

$\tilde{Z}(t)$ denotes the discounted payoff process

$$(23) \qquad \tilde{Z}(t) = \exp(-rt) g(X(t)), \ t \in [0, T].$$

Naturally, evaluating the statement within the infimum of equation (22) with any martingale, $R(t) \in H_0^1$, will give an upper bound to the option price. A martingale, $R^*(t)$, reaching the infimum is called an optimizing martingale. In general, finding an optimizing martingale is as complex as finding the solution to the pricing problem. In fact, when the cost-to-go function, $u_A(t, \boldsymbol{x})$, is known, the optimizing martingale can be written out following the approach in Haugh and Kogan (2004):

$$(24) \qquad \begin{aligned} \mathrm{d}R^*(t) &= \exp(-rt) \left((\nabla u_A)^{\mathrm{T}} \mathbf{b}\right)(t, X(t)) \, \mathrm{d}W(t), \ t \in [0, T], \\ R^*(0) &= 0. \end{aligned}$$

We construct a near-optimal martingale $M^\star \in H_0^1$ by replacing in (24) the exact u_A with the approximate cost-to-go function, $\bar{u}_A$. This yields the explicit upper bound

$$(25) \qquad u_A(0, \boldsymbol{x}_0) \leq \mathrm{E}\left[\sup_{0 \leq t \leq T} \left(\tilde{Z}(q) - R^\star(t)\right) | X(0) = \boldsymbol{x}_0\right],$$

where

$$(26) \qquad \begin{aligned} \mathrm{d}R^\star(t) &= \exp(-rt) \left((\nabla \bar{u}_A)^{\mathrm{T}}(t, \mathbf{P}_1 X(t))\right) \mathbf{P}_1 \mathbf{b}(t, X(t)) \, \mathrm{d}W(t), \ t \in [0, T], \\ R^\star(0) &= 0. \end{aligned}$$

In other words, we evaluate the sensitivity, or delta, of the projected, approximate value function using the projected, non Markovian, version of the true stochastic process. We also note that the sensitivity of the projected, approximate value function can be used as an approximate sensitivity of the option value with regard to the value of the underlying portfolio. (Rogers, 2002, chapter 3)

2.3. **Dimension reduction for models relevant to quantitative finance.** We have established a lower as well as an upper bound for the American basket option prices using Markovian projection. The question of which models feature tight bounds is naturally of interest for the applicability of our methodology. Thus, this section focuses on the domain of applicability of the Markovian projection. Below, we demonstrate that the procedure of Markovian projection produces exact results for the Bachelier Model. This is a consequence of the Gaussian returns in the model. In fact, it turns out that due to the constant volatility (3) of the Bachelier model, the coefficients of the relevant low-dimensional PDEs can be evaluated without Laplace approximation.

Following our discussion about the Bachelier model, we then concentrate on the Black-Scholes model, which is known to produce option prices that are well approximated by the Bachelier model. Finally, we state conditions under which the Black-Scholes model also satisfies the property that the value function of the option depends only on a single state variable s, namely the portfolio value $\mathbf{P}_1 \boldsymbol{x}$.

2.3.1. *Definitions.* First, let us define some terminology. Let $1 \le n < d$ and $D \subset \mathbb{R}^d$ be a convex set with piecewise smooth boundary.

Definition 2.4. We call a function $v : D \to \mathbb{R}$ *essentially n-dimensional* if there exist a function $\zeta : \mathbb{R}^n \to \mathbb{R}$ and a matrix $\mathbf{N} \in \mathbb{R}^{n \times d}$ with orthogonal rows such that $v : \mathbb{R}^d \to \mathbb{R}$ is given by

$$v(\boldsymbol{x}) = \zeta(\mathbf{N}\boldsymbol{x}).$$

Definition 2.5. By extension, we call a differential operator $\mathcal{K}$ essentially n-dimensional if the following backward PDE is well posed

$$
\begin{aligned}
-\partial_t w(t, \boldsymbol{x}) &= \mathcal{K} w(t, \boldsymbol{x}), \quad (t, \boldsymbol{x}) \in [0, T) \times D, \\
w(T, \cdot) &= w_T(\cdot),
\end{aligned}
$$

(27)

and it has an unique essentially n-dimensional solution for any essentially n-dimensional terminal value, w_T. Here we specifically mean that the function ζ may depend on time, that is

$$w(t, \boldsymbol{x}) = \zeta(t, \mathbf{N}\boldsymbol{x}),$$

but the matrix $\mathbf{N}$ does not.

Remark 2.6 (Time independence of lower dimensional subspaces)**.** The definition above rules out solutions to (27) that are essentially lower-dimensional in each instant of time although the directions along which such functions have non-vanishing partial derivatives change over time. We also tacitly assume in this definition that the allowed terminal values make the problem (27) well posed. We later exploit this structure when proving Lemma 2.12 that allows us to reduce the analysis of essentially low-dimensional models to the study of European value functions only, disregarding the possibility for early exercise.

2.3.2. *Bachelier model.* First, we prove that the Markovian projection gives exact results even for American options pricing when used on the Bachelier model. This arises from the fact that the Markovian-projected basket $\overline{S}^{(\boldsymbol{x}_0)}$ coincides in law with the true basket $\mathbf{P}_1 X$. After discussing the one-dimensional nature of the Bachelier model, we propose possible extensions introducing a stochastic clock.

Lemma 2.7 (Dimension reduction in the Bachelier model)**.** *Let $X(t)$ solve* (1) *and the drift and volatility be given by* (2) *and* (3) *respectively. Furthermore, let $\overline{S}^{(\boldsymbol{x}_0)}(t)$ be the Markovian projection defined by eqs.* (11)*,* (12) *and* (13) *for $\mathbf{P}_1 X(t)$. Then $\overline{S}^{(\boldsymbol{x}_0)}(t)$ and $\mathbf{P}_1 X(t)$ coincide in law.*

Proof. The proof is direct. $\square$

We have established that the multivariate Bachelier model has an essentially one-dimensional generator.

However, we know that the model does not feature fat-tailed distribution for returns or clustering of volatility. Both features have been observed in the markets (see Fama (1965) Melino and Turnbull (1991), Mandelbrot (1997) and Cont (2001)). In the following Corollary, we address these issues through the introduction of a stochastic clock. In this way, we introduce a larger class of arbitrage-free dynamics for which the price distribution conditioned to the value of the stochastic clock reduces to the one from the Bachelier model.

Corollary 2.8 (Stochastic time change in the Bachelier model). *Let X be given by the Bachelier model (2, 3) and let $U(t)$ be an almost surely increasing process, or a stochastic clock, independent of X in $\mathbb{R}^+$, with $U(0) = 0$. Let the discounted process corresponding to X be*

$$(28) \qquad \boldsymbol{R}_X(t) = \exp(-rt)\,\boldsymbol{X}(t),$$

then a related stock price process $\boldsymbol{Y}$, given by

$$\boldsymbol{Y}(t) = \exp(rt)\exp(-rU(t))\,\boldsymbol{X}(U(t)) = \exp(rt)\,\boldsymbol{R}_X(U(t))$$

has an essentially one-dimensional generator.

Proof. The proof is divided into two steps.

Step 1. The combination of (28) and (1) yields that $\boldsymbol{R}_X$ is a martingale with respect to its canonical filtration. We show that the same holds for $\boldsymbol{R}_Y(t) = \exp(-rt)\boldsymbol{Y}(t) = \boldsymbol{R}_X(U(t))$.

We take $0 \le s < t \le T$ and consider the conditional expectation

$$
\begin{aligned}
\mathrm{E}\left[\boldsymbol{R}_Y(t)\,|\,\boldsymbol{R}_Y(s)\right] &= \mathrm{E}\left[\boldsymbol{R}_X(U(t))\,|\,\boldsymbol{R}_X(U(s))\right]\\
&= \mathrm{E}\left[\mathrm{E}\left[\boldsymbol{R}_X(U(t))\,|\,\boldsymbol{R}_X(U(s)),U(t),U(s)\right]\,|\,\boldsymbol{R}_X(U(s))\right]\\
&= \mathrm{E}\left[\boldsymbol{R}_X(U(s))\,|\,\boldsymbol{R}_X(U(s))\right]\\
&= \boldsymbol{R}_Y(s).
\end{aligned}
$$

Step 2. Verify the claim of essentially one-dimensionality.

Our goal now is to represent the European option price on the basket $\mathbf{P}_1\boldsymbol{Y}(T)$, w, in terms of a weighted average of European options, each of them written on the basket $\mathbf{P}_1\boldsymbol{X}$.

We have, recalling that $\boldsymbol{Y}(t) = \exp(rt)\exp(-rU(t))\boldsymbol{X}(U(t))$,

$$
\begin{aligned}
(29) \qquad w(t,\boldsymbol{y}) &= \exp(-r(T-t))\mathrm{E}\left[g(\mathbf{P}_1\boldsymbol{Y}(T))\,|\,\boldsymbol{Y}(t)=\boldsymbol{y}\right]\\
&= \exp(-r(T-t))\mathrm{E}\left[\mathrm{E}\left[g(\mathbf{P}_1\boldsymbol{Y}(T))\,|\,U(T),U(t),\boldsymbol{Y}(t)\right]\,|\,\boldsymbol{Y}(t)=\boldsymbol{y}\right]\\
&= \exp(-r(T-t))\mathrm{E}\left[\Pi\,|\,\boldsymbol{Y}(t)=\boldsymbol{y}\right]
\end{aligned}
$$

with

$$\Pi = \mathrm{E}\left[g\left(\exp(-r(U(T)-T))\mathbf{P}_1\boldsymbol{X}(U(T))\right)\,|\,U(T),U(t),\boldsymbol{X}(U(t))\right]$$

being the price of a European option written on the basket $\mathbf{P}_1\boldsymbol{X}$ with maturity time $U(T)$ and time to maturity $U(T)-U(t)$. Then, due to Lemma 2.7, Π is essentially one dimensional and depends only on the basket value

$$\mathbf{P}_1\boldsymbol{X}(U(t)) = \exp(-r(t-U(t)))\mathbf{P}_1\boldsymbol{y},$$

namely

$$(30) \qquad \Pi = h(\mathbf{P}_1\boldsymbol{y}, U(t)-t, U(T)-T).$$

The combination of (29) and (30) thus implies that

$$w(t,\boldsymbol{y}) = \exp(-r(T-t))\mathrm{E}\left[h(\mathbf{P}_1\boldsymbol{y}, U(t)-t, U(T)-T)\right],$$

meaning that w only depends on $\mathbf{P}_1\boldsymbol{y}$, which is what we wanted to prove. □

Remark 2.9 (On the generality of the Stochastic Clock). We note that in proving Corollary 2.8, we allow the stochastic clock U to be quite general.

However, we note that for stochastic clocks with discontinuous trajectories, the dynamics of Y becomes discontinuous and thus the Gyöngy lemma no longer holds. An example of U with continuous trajectories is simply

$$\mathrm{d}U\left(t\right) = \left(c + V^2\left(t\right)\right)\mathrm{d}t,$$
$$U(0) = 0$$

both where $c > 0$ and V is a one-dimensional Ornstein-Uhlenbeck process.

Remark 2.10 (On the density of Bachelier model augmented by stochastic clock)**.** In the preceding discussion above, we have assumed the density of the forward process to be known. For most choices of the stochastic clock process, this assumption will be violated. However, we still have access to the density conditioned on the value of the stochastic clock process. As a result, one may still evaluate the value of the projected volatility, introducing one additional quadrature and integrating over the possible values of the stochastic process.

Remark 2.11 (Stochastic interest rates)**.** For time dependent, stochastic interest rates independent of the price process, one may adopt essentially the same procedure as for the stochastic clock in Corollary 2.8, essentially averaging over possible values for the independent interest rate process.

For other models, such as the Black-Scholes model, there is no guarantee that Markovian projection method for pricing American basket options is exact. However, the similarity of the Black-Scholes and Bachelier models has been pointed out in the simpler European setting in earlier works by Teichmann and others. (Schachermayer and Teichmann, 2008; Grunspan, 2011; Thomson, 2016)

2.3.3. *Other models in reduced dimension.* We have demonstrated that the value function of an American basket option depends only on time and one state variable in the Bachelier model. Here, we present some particular cases in which this property holds for a more general stochastic model. We first show that the reducibility in dimension is a phenomenon, that arises purely from the dynamics of the system, not the early exercise property of the option.

Using this result, we characterize certain parametrizations of the Black-Scholes model that reproduce the reduced dimension behavior familiar from the Bachelier model discussed in the preceding section.

Lemma 2.12 (Decoupling of dimension reduction and early exercise)**.** *If a d-dimensional SDE has a generator $\mathcal{L}$ that is essentially one dimensional, then the corresponding backward operator, $\mathcal{H}$, for the American value function,*

$$(\mathcal{H}v)\left(t,\boldsymbol{x}\right) = (\mathcal{L}v)\left(t,\boldsymbol{x}\right)\mathbf{1}_{\max((\mathcal{L}v)(t,\boldsymbol{x}),\, v(t,\boldsymbol{x})-g(\boldsymbol{x}))>0} \qquad (t,\boldsymbol{x}) \in [0,T] \times D$$

is essentially one dimensional.

Proof. First, define a coordinate rotation, $\mathbf{Q}$, $\mathbf{Q}^{\mathrm{T}}\mathbf{Q} = \mathbf{1}$, such that the portfolio value is given by the first coordinate in the transformed coordinates $\boldsymbol{y} = \mathbf{Q}\boldsymbol{x}$, with $\mathbf{Q}$ chosen so that the first row of $\mathbf{Q}$ and $\mathbf{P}_1{}^{\mathrm{T}}$ are collinear. In these coordinates, denote the Black-Scholes equation for the European value function as

(31)
$$-\partial_t u\left(t,\boldsymbol{y}\right) = \mathcal{L}_y\left(t,\boldsymbol{y}\right)u\left(t,\boldsymbol{y}\right), \left(t,\mathbf{Q}^{\mathrm{T}}\boldsymbol{y}\right) \in [0,T] \times D,$$
$$u\left(T,\boldsymbol{y}\right) = g\left(y_1\right), \mathbf{Q}^{\mathrm{T}}\boldsymbol{y} \in D.$$

To continue the proof, let us consider a Bermudan value function, v_N, with discrete equi-spaced monitoring times, $t_j = \frac{jT}{N}$, $0 \le j \le N$, which solves (Barraquand and Martineau, 1995)

$$-\partial_t v_N(t, \boldsymbol{y}) = \mathcal{L}_y(t, \boldsymbol{y}) v_N(t, \boldsymbol{y}), \quad \left(t, \mathbf{Q}^{\mathrm{T}} \boldsymbol{y}\right) \in (t_i, t_{i+1}) \times D, \ 0 \le i \le N,$$

(32)
$$v_N(T, \boldsymbol{y}) = g(y_1), \quad \mathbf{Q}^{\mathrm{T}} \boldsymbol{y} \in D,$$

$$v_N(t_i, \boldsymbol{y}) = \max\left(v_N(t_i^+, \boldsymbol{y}), g(y_1)\right), \ 0 \le i \le N, \ \mathbf{Q}^{\mathrm{T}} \boldsymbol{y} \in D.$$

The terminal value $g(y_1)$ is essentially one dimensional, and by the assumption on $\mathcal{L}$, we know that $v_N(t, \boldsymbol{y})$ is essentially one dimensional for $t \in (t_{N-1}, t_N)$. Thus, the function $v_N(t_{N-1}, \boldsymbol{y})$ is the maximum of two essentially one-dimensional functions that depend only on the y_1 coordinate. Therefore, we can conclude that

(33)
$$\partial_{y_j} v_N(t_{N-1}, \boldsymbol{y}) = 0, \qquad\qquad j > 1, \ \mathbf{Q}^{\mathrm{T}} \boldsymbol{y} \in D$$

and, by using the same argument for all the subsequent intervals (t_{i-1}, t_i), we have that

(34)
$$\partial_{y_j} v_N(t, \boldsymbol{y}) = 0, \qquad\qquad j > 1, \ \mathbf{Q}^{\mathrm{T}} \boldsymbol{y} \in D, \ \forall t \in [0, T].$$

The American option value function, v, solves

$$-\partial_t v(t, \boldsymbol{y}) = \mathcal{H}_y(t, \boldsymbol{y}) v(t, \boldsymbol{y}), \qquad\qquad \left(t, \mathbf{Q}^{\mathrm{T}} \boldsymbol{y}\right) \in [0, T] \times D,$$

$$v(T, \boldsymbol{y}) = g(y_1), \qquad\qquad \mathbf{Q}^{\mathrm{T}} \boldsymbol{y} \in D,$$

where $\mathcal{H}_y$ is the $\boldsymbol{y}$-coordinate representation of the operator defined in equation (9). v is given as the limit of Bermudan value functions as the number of exercising times, N, tends to infinity:

(35)
$$v(t, \boldsymbol{y}) = \lim_{N \to \infty} v_N(t, \boldsymbol{y}), \qquad\qquad \left(t, \mathbf{Q}^{\mathrm{T}} \boldsymbol{y}\right) \in [0, T] \times D.$$

The combination of (34) and (35) yields

$$\partial_{y_j} v(t, \boldsymbol{y}) = 0, \qquad\qquad j > 1, \ \mathbf{Q}^{\mathrm{T}} \boldsymbol{y} \in D, \ \forall t \in [0, T],$$

which concludes the proof. $\qquad\qquad\qquad\qquad\qquad\qquad\qquad\qquad\qquad\qquad\qquad$ $\square$

We have already seen that the Bachelier model is one example, in which the Hamiltonian operator, $\mathcal{H}$, is essentially one-dimensional. Next, we proceed to other examples of stochastic models where the generator $\mathcal{L}$ is essentially one-dimensional, guaranteeing dimension reduction in the American option value function.

2.3.4. *Black-Scholes model.* Next, we turn our focus to the Black-Scholes model itself and examine how it behaves under Markovian projection and whether there exist parametrizations of the model that are essentially one dimensional.

First, let us state the relevant Black-Scholes PDE (6) corresponding to the Black-Scholes model:

(36)

$$-\partial_t w(t, \boldsymbol{x}) = \underbrace{-rw(t, \boldsymbol{x}) + r \sum_i x_i \partial_{x_i} w(t, \boldsymbol{x}) + \sum_{ij} \Omega_{ij} x_i x_j \partial^2_{x_i x_j} w(t, \boldsymbol{x})}_{\equiv (\mathcal{L}_{BS} w)(t, \boldsymbol{x})}, \ t \in [0, T], \ \boldsymbol{x} \in D^d_{BS},$$

$$w(T, \cdot) = g(\mathbf{P}_1 \cdot),$$

where the symmetric matrix, $\boldsymbol{\Omega} \in \mathbb{R}^{d \times d}$, is understood as the quadratic form corresponding to a volatility matrix, $\boldsymbol{\Sigma} \in \mathbb{R}^{d \times k}$, of equation (4), $\boldsymbol{\Omega} = \frac{\boldsymbol{\Sigma}\boldsymbol{\Sigma}^{\mathrm{T}}}{2}$. The domain is given as $D = D^d_{BS} = \mathbb{R}^d_+$

Remark 2.13. A trivial example of a parametrization of the Black-Scholes model for which the value function is essentially one-dimensional is the case when portfolio weights vanish except for one, $\mathbf{P}_1 = [1, 0, 0, \ldots, 0, 0]$. For such a portfolio, we can write a one-dimensional PDE describing the cost-to-go function.

For an arbitrary set of portfolio weights, $\mathbf{P}_1$, of the Black-Scholes model Remark 2.13 certainly does not apply. However, we may apply a coordinate transformation to transform the portfolio weights to the particular choice in Remark 2.13. If the resulting transformed PDE is of the form (36), this is sufficient to show that the value function is essentially one-dimensional.

Below, we demonstrate this and give a particular class of parametrizations, for which the transformation is possible. For other parametrizations, we note that these parametrizations can be approximated by ones where portfolio returns are log-normal. For a discussion of approximating the linear combination of variables from a multivariate log-normal, we refer the reader to Mehta *et al.* (2007).

We rotate the coordinates of the Black-Scholes equation (36) using the coordinate transformation, $\mathbf{Q}$, from the proof of Lemma 2.12. We have

$$
\begin{aligned}
\mathcal{L}_{BS,y} u(t, \boldsymbol{y}) = & -r u(t, \boldsymbol{y}) \\
& + r \sum_{ikl} Q_{ki} Q_{il} y_k \partial_{y_l} u(t, \boldsymbol{y}) \\
& + \sum_{ijklmn} \Omega_{ij} Q_{ki} Q_{lj} Q_{jm} Q_{in} y_k y_l \partial^2_{y_m y_n} u(t, \boldsymbol{y}), \qquad t \in [0, T], \ \mathbf{Q}^{\mathsf{T}} \boldsymbol{y} \in D_{BS}^d.
\end{aligned}
$$

Thanks to the orthogonality of the transformation matrix $\mathbf{Q}$, the first-order operator simplifies to

$$
\sum_{ikl} \underbrace{Q_{kl} Q_{il}}_{=\delta_{ik}} y_k \partial_{y_l} u(t, \boldsymbol{y}) = \sum_i y_i \partial_{y_i} u(t, \boldsymbol{y}).
$$

However, the transformed second-order term does not take the form given in (36) in the general case. By writing in a tensorized form

$$
(37) \qquad \sum_{ijklmn} \Omega_{ij} Q_{ki} Q_{lj} Q_{jm} Q_{in} y_k y_l \partial^2_{y_m y_n} u(t, \boldsymbol{y}) = \Gamma_{klmn} y_k y_l \partial^2_{y_m y_n} u(t, \boldsymbol{y})
$$

we have that $\boldsymbol{\Gamma}$ has in general non-diagonal terms that couple y_k and y_l to $\partial^2_{y_m y_n} u$ for $\{k, l\} \neq \{m, n\}$. Another way to write the second-order term is

$$
\mathrm{Tr}\left(\boldsymbol{\Omega} \mathrm{diag}\left(\mathbf{Q}^{\mathsf{T}} \boldsymbol{y}\right)\left(\mathbf{Q}^{\mathsf{T}} (\mathbf{H}u) \mathbf{Q}\right) \mathrm{diag}\left(\mathbf{Q}^{\mathsf{T}} \boldsymbol{y}\right)\right).
$$

Using this notation, we give a particular example of a class of parametrizations of the Black-Scholes model for which the second-order term has the diagonal structure such that the generator $\mathcal{L}_{BS}$ is essentially one-dimensional.

Corollary 2.14 (Effective one-dimensionality of Black-Scholes model when the quadratic form has equal elements)**.** *A Black-Scholes model such that the quadratic form in equation (36) satisfies $\Omega_{ij} = C$ for $1 \leq i, j \leq d$ has an essentially one-dimensional generator.*

Proof. The proof is direct. Writing out the second-order term (37) we get

$$\sum_{ijklmn} \Omega_{ij} Q_{ki} Q_{lj} Q_{jm} Q_{in} y_k y_l \partial^2_{y_m y_n} u(t, \mathbf{y})$$

$$= C \sum_{iklmn} Q_{ki} \underbrace{\left(\sum_j Q_{lj} Q_{jm} \right)}_{\delta_{lm}} Q_{in} y_k y_l \partial^2_{y_m y_n} u(t, \mathbf{y})$$

$$= C \sum_{klmn} \delta_{lm} \underbrace{\left(\sum_i Q_{ki} Q_{in} \right)}_{\delta_{kn}} y_k y_l \partial^2_{y_m y_n} u(t, \mathbf{y})$$

$$= C \sum_{klmn} \delta_{kn} \delta_{lm} y_k y_l \partial^2_{y_m y_n} u(t, \mathbf{y})$$

$$= C \sum_{kl} y_k y_l \partial^2_{y_k y_l} u(t, \mathbf{y}).$$

$\square$

We have demonstrated that there is a non-trivial set of parametrizations of the Black-Scholes model such that their corresponding generators $\mathcal{L}_{BS}$ are essentially one-dimensional.

For parametrizations that are not essentially one-dimensional, we still note that the upper and lower bounds (21) and (25) still hold. However, there is no a priori reason to believe that they coincide. In the next section, we evaluate the bound for a range of parametrizations and argue that these bounds are often close enough to get a practical estimate of the option price. This is expected due to the Multivariate Black-Scholes model being well approximated by an univariate Black-Scholes model on the one hand and the multivariate Bachelier model on the other. We have established above that the Markovian projection works for pricing in both the multivariate Bachlier model as well as the univariate Black-Scholes model. We demonstrate that this property carries over to the multivariate Black-Scholes model as a good approximation.

3. Numerical implementation

Here, we present a numerical implementation of our proposed method. First, we describe in Section 3.1 the methods used to evaluate the coefficients of the relevant PDE (18) in $\overline{D}$. We briefly introduce the solution of the projected HJB equation in Section 3.2 and proceed in Section 3.3 to describe the evaluation of the lower and upper bounds using forward-Euler Monte Carlo simulation. We finally discuss the errors arising in the numerical methods in Section 3.4 and apply the proposed methods to Bachelier and Black-Scholes models of relevance in Section 3.5

3.1. **Evaluation of local volatility.** So far, we have bypassed the issue of how to evaluate the local projected volatility $\overline{b}^{(x_0)}$ in equation (13). In this section we first describe in Section 3.1.1 how we may efficiently evaluate the high-dimensional integrals involved in the definition of the projected volatility $\overline{b}^{(x_0)}$. This discussion is followed by an interpolation scheme for extending pointwise evaluations of $\overline{b}^{(x_0)}$ into the projected domain $\overline{D}$ in Section 3.1.2.

3.1.1. *Laplace approximation.* To approximate u_A with $\bar{u}_A$, we must efficiently evaluate the conditional expectations (12) and (13) that involve high-dimensional integrals. For the risk-neutral case (2) that is of most interest in financial applications and options pricing, the drift part will trivially project as

$$
\begin{aligned}
\bar{a}^{(x_0)}(t,s) &= \mathrm{E}\left[\mathbf{P}_1 a\left(t, X(t)\right) | \mathbf{P}_1 X(t) = s, \ X(0) = x_0\right] \\
&= \mathrm{E}\left[\mathbf{P}_1\left(r X(t)\right) | \mathbf{P}_1 X(t) = s, \ X(0) = x_0\right] \\
&= rs.
\end{aligned}
$$

For the volatility, $\bar{b}^{(x_0)}$, we employ the Laplace approximation, by essentially finding an extremal point of the relevant unimodal integrands and applying a second-order approximation around that extremal point. Along this line, we make the following assumption.

Assumption 3.1. We assume that the transition density from x_0 to y $\phi(y; x_0)$ $\phi : \mathbb{R}^d \to \mathbb{R}$ corresponding to the process (1) is a smooth function for $0 \le t \le T$ and it is known explicitly.

The precise implementation of this approximation can be done in various ways, but the underlying principle remains the same. Some of these approaches allow to relax Assumption 3.1. Below we outline the Laplace approximation for the case where the assumption holds. For a more detailed account of the use of Laplace approximation, we refer the reader to Shun and McCullagh (1995) and Goutis and Casella (1999).

Let

$$
\gamma(s) = \mathrm{E}\left[\Psi(X(t)) | \mathbf{P}_1 X(t) = s, \ X(0) = x_0\right],
$$

with $\Psi(X(t)) \in L^2(\mathbb{R})$. Then, this conditional expectation satisfies

(38) $\qquad \mathrm{E}\left[\Psi(X(t))\theta(\mathbf{P}_1 X(t)) | X(0) = x_0\right] = \mathrm{E}\left[\gamma(\mathbf{P}_1 X(t))\theta(\mathbf{P}_1 X(t)) | X(0) = x_0\right],$

for all θ such that $\theta(\mathbf{P}_1 \cdot) \in L^2(\mathbb{R})$. Taking in (38) $\theta_h(x) = \frac{1}{h}\mathbf{1}_{2|x-s|<h}$ for $h > 0$ and letting $h \to 0^+$ the left-hand of the previous identity becomes a surface integral over a hyperplane

$$
\lim_{h\to 0^+}\mathrm{E}\left[\Psi(X(t))\theta_h(\mathbf{P}_1 X(t))\right] = \int_{\mathbf{P}_1 x = s}\Psi(x)\phi(x; x_0)\,\mathrm{d}A(x),
$$

where $\mathrm{d}A$ denotes the differential element of the hyperplane. For the right-hand side we have similarly

$$
\lim_{h\to 0^+}\mathrm{E}\left[\gamma(\mathbf{P}_1 X(t))\theta_h(\mathbf{P}_1 X(t))\right] = \gamma(s)\int_{\mathbf{P}_1 x = s}\phi(x; x_0)\,\mathrm{d}A(x).
$$

Setting $\Psi(\cdot) = \mathbf{P}_1 \mathbf{b}\mathbf{b}^{\mathrm{T}}\mathbf{P}_1^{\mathrm{T}}(t, \cdot)$ and solving for $\gamma(s)$ in (38), we have

(39) $\qquad \left(\bar{b}^{(x_0)}\right)^2(t,s) = \dfrac{\int_{\mathbb{R}^{d-1}}\phi(x(z); x_0)\left(\mathbf{P}_1 \mathbf{b}\mathbf{b}^{\mathrm{T}}\mathbf{P}_1^{\mathrm{T}}\right)(t, x(z))\,\mathrm{d}z}{\int_{\mathbb{R}^{d-1}}\phi(x(z); x_0)\,\mathrm{d}z},$

where we treat the first variable of x above as the dependent variable,

$$
x_i(z) = z_i, \ \forall i > 1,
$$

$$
x_1(z) = (P_{11})^{-1}\left(s - \sum_{j=2}^{d}P_{1j}z_j\right).
$$

Emphasizing that we work in $\mathbb{R}^d$, rather than the possibly bounded domain D, we approximate the integrals in equation (39), using Laplace approximation. We replace the

unimodal integrands by suitable Gaussian functions centered at their maximizing configu-
rations, $z^* \in \mathbb{R}^{d-1}$ and $z^\star \in \mathbb{R}^{d-1}$.

Denoting the integrand by $\exp(f)$ and exploiting the negative-definiteness of the Hes-
sian $\mathbf{H}f$, we may then approximate the integrand by expanding its logarithm f as follows.

$$
\int_{\mathbb{R}^{d-1}} \exp(f(z)) \, \mathrm{d}z \approx \int_{\mathbb{R}^{d-1}} \exp\left(f(z^*) + \frac{(z - z^*)^T (\mathbf{H}f)(z^*)(z - z^*)}{2} \right) \mathrm{d}z
$$

(40)
$$
= \exp(f(z^*)) \sqrt{\frac{(2\pi)^{d-1}}{\det|(\mathbf{H}f)(z^*)|}}.
$$

We employ the same approximation for both the denominator and the numerator of equa-
tion (39) and get

(41)
$$
\frac{\int_{\mathbb{R}^{d-1}} \exp(f(z)) \, \mathrm{d}z}{\int_{\mathbb{R}^{d-1}} \exp\left(\tilde{f}(z)\right) \mathrm{d}z} \approx \exp\left(f(z^*) - \tilde{f}\left(z^\star\right) \right) \sqrt{\frac{\det\left|\left(\mathbf{H}\tilde{f}\right)(z^\star)\right|}{\det|(\mathbf{H}f)(z^*)|}} \equiv \tilde{b}_1^2(t, s),
$$

where

$$
\tilde{f}(z) = \log\left(\phi(x(z) ; x_0)\right)
$$
$$
f(z) = \log\left(\phi(x(z) ; x_0) \, \mathbf{P}_1 \mathbf{b}\mathbf{b}^{\mathrm{T}} \mathbf{P}_1{}^{\mathrm{T}}(t, x(z))\right)
$$

and $z^\star$ and z^* are the critical points for $\tilde{f}$ and f respectively.

In practice, the critical configurations can be found rapidly by expanding the known
integrand, f, to second order and applying the Newton's iteration scheme,

(42)
$$
z^{(n+1)} = \left(\mathbf{H}f\left(z^{(n)}\right)\right)^{-1} \nabla f\left(z^{(n)}\right).
$$

The iteration quickly converges to an extremal point, typically within a few dozens of
iterations allowing fast evaluation. Note that in the case of the Black-Scholes model, the
density ϕ contains a quadratic term, which makes the Newton iteration very robust to the
choice of initial configuration $z^{(0)}$ in (42).

We note that the approximation is rather simple for the case where the density of the
process is normal or log-normal, i.e. the original process (1) corresponds to Bachelier or
Black-Scholes model. Bayer and Laurence (2014) consider the CEV model using the heat
kernel approximation (see, for example, Yosida (1953)) for the transition density.

For numerical results on the accuracy of the Laplace approximation, we refer the reader
to Appendix A, where the alternate choices of coordinates for the second-order expansion
are discussed, along with their respective accuracies.

3.1.2. *Extrapolation-interpolation to projected domain.* To solve for the projected cost-to-
go function, $\overline{u}_A(t, s)$ in equation (18), we use the Laplace approximation introduced above
to evaluate the projected local volatility in a few points in the domain, $\overline{D}$. We extend these
values to a truncated domain in which we solve the low dimensional equation (18). Thanks
to the smooth behavior of the the projected volatility, $\overline{b}^{(x_0)}$, we only need a relatively low
number of evaluations to achieve high accuracy.

However, to verify that the resulting projected cost-to-go function $\overline{u}_A$ is indeed a good
approximation of u_A using the lower and upper bounds requires Monte Carlo simulation,
which is typically costly compared to the solution of the projected backward problem (44).

To evaluate the projected volatility, $\overline{b}^{(x_0)}$, we generate a small Monte Carlo forward-
Euler sample of trajectories of the original process (1), as $X(t_n, \omega_i)$, $0 \le t_n \le N_t$ and
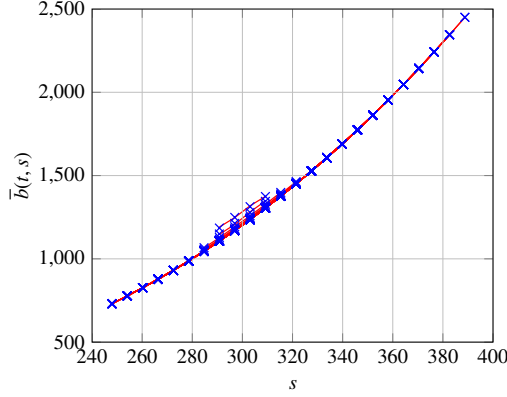
(a) Third-order polynomial interpolation for the three-dimensional Black-Scholes model. Each red line corresponds to an instant of time from 0 to $T = \frac{1}{2}$ and is obtained through regression of a corresponding set of evaluations indicated through blue crosses.
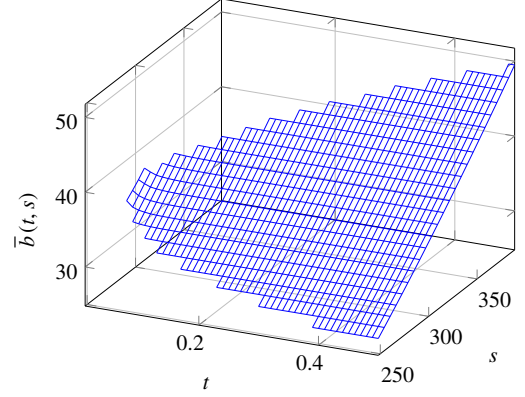
(b) Local volatility for the projected dynamics in the high likelihood region of the 3-to-1 dimension equation (56). For the corresponding implied volatilities, see Figure 2(b)

FIGURE 1. Projected volatility $\tilde{b}_1 (t, s)$ of equation (41) and its interpolation in space and time for the 3-to-1 dimensional Black-Scholes model (56). In both the figures, the plots are done for the range of essential support of the density, which expands as t increases.

$1 \le i \le M$ for $M \approx 100$, and to evaluate the essential support $[S^-(t_n), S^+(t_n)] \subset \overline{D}$ of the basket process that satisfies

(43)
$$S^-(t_n) = \min_i \mathbf{P}_1 X(t_n, \omega_i) \ 0 \le n \le N_t, \ 1 \le i \le M,$$
$$S^+(t_n) = \max_i \mathbf{P}_1 X(t_n, \omega_i) \ 0 \le n \le N_t, \ 1 \le i \le M.$$

We select a few dozen points equispaced in the intervals $[S^-(t_n), S^+(t_n)]$ for each time step t_n and create a polynomial fit for $\overline{b}^{(x_0)}$ for each of these instances of time.

Remark 3.2. We note that the projected volatility can only be reliably evaluated inside the area where the density for $\mathbf{P}_1 X(t)$ is not negligible. At the most extreme case, at the initial time, the density of $\mathbf{P}_1 X(0)$ focuses on a single point. In reality, the appropriate domain for $\overline{D}$ has the schematic shape depicted in Figure 1(b). However, we carry out our evaluation of $\overline{u}_A$ in a rectangular domain $[0, T] \times \overline{D}$ and extrapolate the local volatility into the whole rectangle. In carrying out the extrapolation, we set a small minimum value for $\left(\overline{b}^{(x_0)}\right)^2$ to guarantee numerical stability in the backward solver.

Note that the envelope (43) is only used to get a rough estimate of where the probability mass of $\mathbf{P}_1 X(t)$ for $0 \le t \le T$ lies and has a very indirect effect on the numerical solution as such. The resulting numbers of time steps N_t and samples M invested in (43) are small in comparison to the forward-Euler solution of the upper and lower bounds discussed later in Section 3.3.

3.2. **Numerical value function.** Once we define the interpolated-extrapolated approximate projected volatility $\tilde{b}$ by interpolating the approximate projected volatility in equation (39), we set to define a finite-difference approximation $\overline{\overline{u}}_A$ of the value function $\overline{u}_A$ that

solves equation (18). Based on the finite difference operator

$$\left(\overline{\overline{\mathcal{L}u}}\right)(t, s_n)$$

$$= \left(\frac{\tilde{b}^2(t, s_n)}{2\Delta s^2} + \frac{r s_n}{2\Delta s}\right)\overline{\overline{u}}(t, s_{n-1}) - \left(r + \frac{\tilde{b}^2(t, s_n)}{\Delta s^2}\right)\overline{\overline{u}}(t, s_n) + \left(\frac{\tilde{b}^2(t, s_n)}{2\Delta s^2} - \frac{r s_n}{2\Delta s}\right)\overline{\overline{u}}(t, s_{n+1}),$$

$$1 < n < N_s,$$

that parallels (Merton *et al.*, 1977, equation (12)) and whose continuous counterpart is $\overline{\mathcal{L}}$ of equation (16), we use a stable backward Euler scheme,

$$
\begin{aligned}
&\overline{\overline{u}}_A\left(t_{n-1}^+, s_m\right) = \overline{\overline{u}}_A(t_n, s_m) + \left(\overline{\overline{\mathcal{L}u}}\right)\left(t_{n-1}^+, s_m\right)\Delta t_n,\ 1 \le n \le N_t,\ 1 \le m \le N_s,\\
(44)\qquad &\overline{\overline{u}}_A(t_{n-1}, s_m) = \max\left(\overline{\overline{u}}_A\left(t_{n-1}^+, s_m\right), g(s_m)\right),\ 1 \le n \le N_t,\ 1 \le m \le N_s,\\
&\overline{\overline{u}}_A(t_{N_t}, sm) = g(s_m)\ 1 \le m \le N_s,
\end{aligned}
$$

with the artificial Dirichlet-type boundary condition (see Remark 2.2) imposed by the pay-off

$$
(45)\qquad
\begin{aligned}
\overline{\overline{u}}_A(t_n, s_1) &= g(s_1),\\
\overline{\overline{u}}_A(t_n, s_{N_s}) &= g(s_{N_s})
\end{aligned}
$$

and a homogeneously spaced, time-independent, mesh $s_m = m\Delta s$. The choice of the boundary condition has been discussed in the variational setting by (Feng *et al.*, 2007, pp. 316). The upper bound s_{N_s} has to be chosen based on the magnitude of the drift and the volatility for the problem at hand.

The pointwise value function is later extended to the whole domain $\overline{D}$ of equation (36) using a low order interpolant, allowing the evaluation of a discrete early exercise region

$$(46)\qquad \overline{D}_{\mathrm{Ex}} = \left\{(t_n, s_m) : 0 \le n \le N_T,\ 1 \le m \le N_s, \overline{\overline{u}}_A(t_n, s_m) = g(s_m)\right\}$$

Similarly, for the construction of the dual bound given by equation (26), we approximate derivatives of $\overline{u}_A$ (eq. (36)) using finite differences of $\overline{\overline{u}}_A$ (eq. (44)).

3.3. **Forward-Euler approximation.** The discrete American put option value $\overline{\overline{u}}_A$ that solves the backward-Euler scheme (44) implies a corresponding discrete early exercise region $\overline{D}_{\mathrm{Ex}}$ of equation (46).

To verify the accuracy of the early exercise boundary implied by the discrete option value $\overline{\overline{u}}_A$ as an approximation to the exercise boundary in u_A and to set a confidence interval for the option price, we evaluate the lower and upper bounds in equations (21) and (26) using Monte Carlo simulations based on (Forward) Euler-Maruyama. The numerical time-stepping for the asset prices, $X(t)$, is done on a uniform mesh. Setting the total number of time steps to coincide with the ones used in the finite difference approximation of $\overline{\overline{u}}_A$ defined in (44), avoids the need for temporal interpolation of $\overline{\overline{u}}_A$. As mentioned above, we use the following discretization of equation (1):

$$
(47)\qquad
\begin{aligned}
\overline{\overline{X}}(t_{n+1}) &= \overline{\overline{X}}(t_n) + r\overline{\overline{X}}(t_n)\Delta t_n + \mathbf{b}\left(t_n, \overline{\overline{X}}(t_n)\right)\Delta W(t_n),\ 0 \le n < N_t,\\
\overline{\overline{X}}(t_0) &= \mathbf{x},
\end{aligned}
$$

with $\Delta t_n = t_{n+1} - t_n$ and $\Delta W(t_n) = W(t_{n+1}) - W(t_n) \sim \mathcal{N}(0, t_{n+1} - t_n)$ and the number of time steps N_t. Correspondingly, we approximate equation (23) as

$$
(48) \qquad \overline{\overline{Z}}(t_n) = \exp(-rt_n) g\left(\mathbf{P}_1 \overline{\overline{X}}(t_n)\right), \qquad\qquad 0 \le n < N_t.
$$

We use the same underlying Brownian motion to generate approximate trajectories for both the asset $\overline{\overline{X}}$ and the approximation to the martingale R in equation (26) used to construct the upper bound for the option price:

$$
\overline{\overline{R}}(t_{n+1}) = \overline{\overline{R}}(t_n) + \exp(-rt_n)\left(\overline{\overline{\nabla u}}_A\right)^{\mathrm{T}}\left(t_n, \mathbf{P}_1\overline{\overline{X}}(t_n)\right)\mathbf{b}\left(t_n, \overline{\overline{X}}t\right)\Delta W(t_n),
$$

$$
(49) \qquad\qquad 0 \le n < N_t,
$$

$$
\overline{\overline{R}}(0) = 0.
$$

With the discrete approximations (47) and (49), we can estimate an upper bound, A^+, and a lower bound, A^-, for the option price, $u_A(0, X(0))$, using sample averages of M i.i.d samples, namely

$$
(50) \qquad
\begin{aligned}
A^+_{M,N_t} &= \frac{1}{M} \sum_{i=1}^{M} u^+(\omega_i), \\[2mm]
u^+ &= \max_{0 \le j \le N_t}\left(\overline{\overline{Z}}(t_j) - \overline{\overline{R}}(t_j)\right)
\end{aligned}
$$

and

$$
(51) \qquad
\begin{aligned}
A^-_{M,N_t} &= \frac{1}{M} \sum_{i=1}^{M} u^-(\omega_i), \\[2mm]
u^- &= \exp\left(-r\overline{\overline{\tau}}\right) g\left(\mathbf{P}_1 \overline{\overline{X}}\left(\overline{\overline{\tau}}\right)\right), \\[2mm]
\partial\overline{D}_{\mathrm{Ex.}}(t_n) &= \max\left\{1 \le m \le N_s : (t_n, s_m) \in \overline{D}_{\mathrm{Ex.}}\right\} \\[2mm]
\overline{\overline{\tau}} &= \min\left\{0 \le j \le N_t : \mathbf{P}_1\overline{\overline{X}}(t_j) \le \partial\overline{D}_{\mathrm{Ex.}(t_n)}\right\}.
\end{aligned}
$$

To estimate the bias in the discretized approximations of the price bounds, we generate Monte Carlo samples corresponding to different values of N_t and estimate the difference between the resulting estimators, $\left|A^+_{M,2N_t} - A^+_{M,N_t}\right|$ and $\left|A^-_{M,2N_t} - A^-_{M,N_t}\right|$. For a discussion on using the forward-Euler scheme for evaluating hitting times as the one in equation (51), we refer the reader to Buchmann (2003); Bayer *et al.* (2010)

In order to accelerate the computations of the bounds, we note the possibility of using multilevel estimators instead of those in (51) and (50) (Giles, 2015). This is out of the scope of this work.

In Section 3.5, we present a selected set of test cases for which we evaluate the estimators (50) and (51). We focus in particular on the multivariate Black-Scholes that is both relevant and non-trivial and satisfies Assumption 3.1. The parametrizations of the Black-Scholes model we study do not feature essentially one-dimensional value functions and thus serve as a test case of our method when the accuracy of the method is not guaranteed a priori. Still, using the lower and upper bounds, we can analyze the accuracy of our method and verify its accuracy. For verification purposes, we include tests on the constant-volatility Bachelier model, for which the Markovian projection reproduces the American option prices exactly.

3.4. **Error decomposition.** Before proceeding further into the numerical examples we provide a brief summary of the errors incurred in the numerical solution of our price bounds, decomposing the total error into its constituent parts. Denoting the estimators of equations (50) and (51) as

$$A^{\pm}_{\infty,\infty} = \lim_{M,N_t \to \infty} A^{\pm}_{M,N_t},$$

we have that the option price u_A satisfies

$$A^{-}_{\infty,\infty} \leq u_A(0,\boldsymbol{x}) \leq A^{+}_{\infty,\infty}.$$

In practice, we rely on estimators based on finite M and N_t. The magnitude of the gap $\left|A^{+}_{\infty,\infty} - A^{-}_{\infty,\infty}\right|$ is dictated by the approximate value function $\bar{u}_A$ that gives rise to the inexact stopping time (20) as well as the dual martingale M. In general, finding an approximate function $\bar{u}_A$ that approximates the true solution u_A closely might not be possible. Furthermore, even when a sound one-dimensional approximation $\bar{u}_A$ exists, we rely on an approximate integration formula to recover it. Thus, for a general model, we are not able to control the error of our method and the magnitude of the gap $\left|A^{+}_{\infty,\infty} - A^{-}_{\infty,\infty}\right|$. However, we are interested in choosing numerical parameters such that we get a reliable and useful estimate of the magnitude of this gap.

In addition to the gap between $A^{+}_{\infty,\infty}$ and $A^{-}_{\infty,\infty}$, the difference between $A^{\pm}_{\infty,\infty}$ and the corresponding estimators $A^{\pm}_{M,N_t}$ is of interest. Below, we outline the numerical approximations that give rise to these differences. Besides the fundamental error implied by approximating τ^* of equation (19) with $\bar{\tau}^{\dagger}$ of equation (20),there are four main numerical approximations employed in the procedure, with each of them giving rise to a distinct component to the error. These are:

(1) the statistical error due to finite number of samples, M, in (50) and (51),
(2) the step size bias introduced in the forward-Euler approximation (47),
(3) the discretization errors of the solution $\bar{u}$, giving rise to inexact approximations to the early-exercise region and the sensitivity in equation (49)
(4) the Laplace approximation error when evaluating the integrals for the coefficients of the projected dynamics and the corresponding backward solution in equation (40).

Noting that the choice of the time-stepping scheme implies an optimal dependence between the number of temporal and spatial discretization steps, N_t and N_s, and using the optimal N_s, we expand the notation for the estimators A^{-} and A^{+} to

$$A^{\pm}_{M,N_t} = A^{\pm}_{M,N_t,N_t,\tilde{b}_1},$$

where the first N_t refers to the number of forward-Euler time steps and the latter to the corresponding steps in the backward solver. With the triangle inequality, we decompose

$$\left|A^{\pm}_{\infty,\infty} - A^{\pm}_{M,N_t}\right| = \left|A^{\pm}_{\infty,\infty,\infty,\bar{b}(x_0)} - A^{\pm}_{M,N_t,N_t,\tilde{b}_1}\right|$$

$$\leq \left|A^{\pm}_{\infty,\infty,\infty,\bar{b}(x_0)} - A^{\pm}_{\infty,\infty,\infty,\tilde{b}_1}\right| + \left|A^{\pm}_{\infty,\infty,\infty,\tilde{b}_1} - A^{\pm}_{\infty,\infty,N_t,\tilde{b}_1}\right|$$

$$+ \left|A^{\pm}_{\infty,\infty,N_t,\tilde{b}_1} - A^{\pm}_{\infty,N_t,N_t,\tilde{b}_1}\right| + \left|A^{\pm}_{\infty,N_t,N_t,\tilde{b}_1} - A^{\pm}_{M,N_t,N_t,\tilde{b}_1}\right|.$$

For the Laplace error $\left|A^{\pm}_{\infty,\infty,\infty,\bar{b}(x_0)} - A^{\pm}_{\infty,\infty,\infty,\tilde{b}_1}\right|$, there is no simple and practical way to control the error. We estimate the error through the numerical experiments as presented in the appendix A. All the other components are well defined and can be controlled using
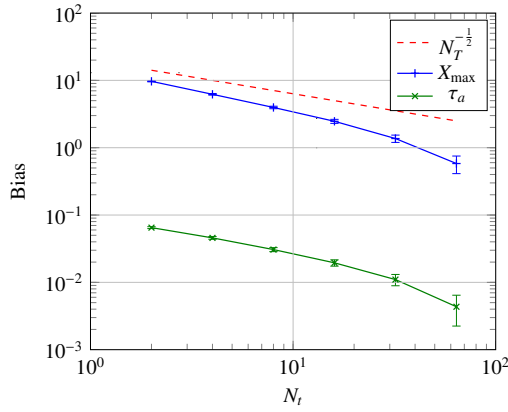
(a) Convergence of the expected hitting time (τ_a, green) to the early exercise region and the expected maximum ($X_{\max}$, blue) over the interval $0 \leq t \leq \frac{1}{2}$ for a 3-dimensional correlated Black-Scholes model (56) along with the $N_t^{-\frac{1}{2}}$ reference line (dashed red).
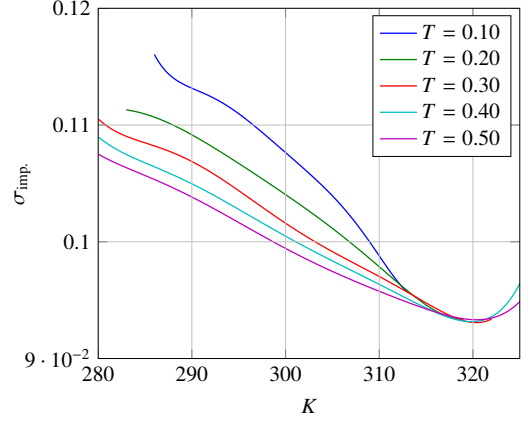
(b) The implied volatility for the American put option corresponding to the local volatility of the projected 3-dimensional Black-Scholes model (56). Each of the values for $\sigma_{\text{imp.}}$ produces the option prices for their respective strike price, K, for the American option price, when the local volatility is given by the projected dynamics.

FIGURE 2

standard arguments in their respective numerical methods. Firstly, with regard to the finite sample size, we can, given a confidence parameter, exploit the central limit theorem (CLT) and control the statistical error in probability by increasing the sample size,

$$(52) \qquad \left| A^{\pm}_{\infty,N_t,N_t,\tilde{b}_1} - A^{\pm}_{M,N_t,N_t,\tilde{b}_1} \right| = O_P\left(M^{-\frac{1}{2}}\right).$$

As for the temporal discretization parameter, for the backward-Euler method, we set N_s in equation (44) to $N_s^2 = cN_t$, giving rise to the discretization error,

$$(53) \qquad \left| A^{\pm}_{\infty,\infty,\infty,\tilde{b}_1} - A^{\pm}_{\infty,\infty,N_t,\tilde{b}_1} \right| = O\left(N_t^{-1}\right).$$

Finally, for the simulation of the extremal point of the dual martingale in equation (26) and the hitting time into the early exercise region implied by $\overline{u}_A$, we have

$$(54) \qquad \left| A^{\pm}_{\infty,\infty,N_t,\tilde{b}_1} - A^{\pm}_{\infty,N_t,N_t,\tilde{b}_1} \right| = O\left(N_t^{-\frac{1}{2}}\right),$$

for each, as shown in Figure 2(a).

The novel contribution of this work is the use of the projected process for determining an implied exercise strategy for the true pricing problem (7) using the projected value function $\overline{u}_A$ that solves (18). In the following sections, we wish to demonstrate the feasibility of this approach, and measure the resulting error, choosing parameters such that the errors (52), (53) and (54) are small compared to the error implied by the use of the surrogate process and its approximate evaluation using Laplace approximation. We proceed to do this in the following section.

3.5. **Examples.** This section demonstrates the performance of our proposed method for pricing American put options written on a basket. First, we verify our results using a
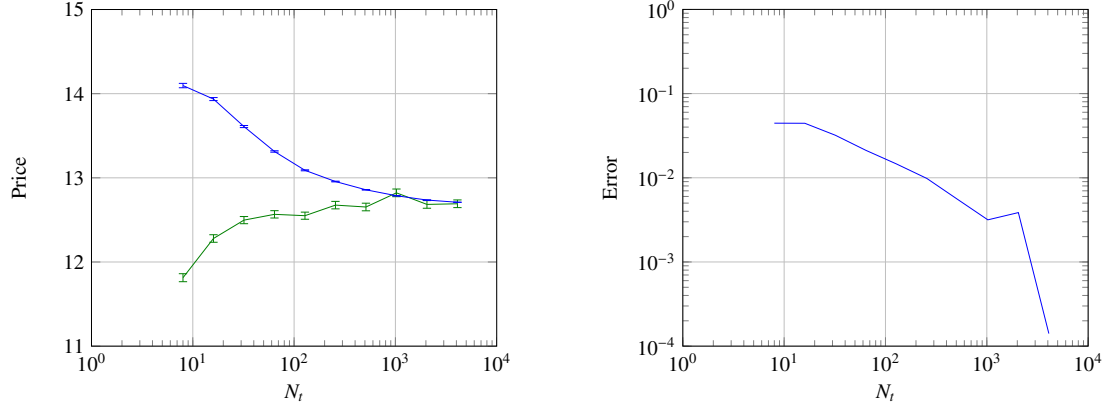
(a) The upper A^+_{128000,N_t} (Blue) and lower bound A^-_{128000,N_t} (Green) for the American put price for varying numbers of time steps, N_t, in the forward-Euler discretization. Error bounds correspond to 95 percent confidence level. For the corresponding behavior of the relative width of the confidence interval, see Figure 3(b).

(b) The distance of the error bounds relative to the underlying option price for the at-the-money put for the test case presented in Figure 3(a). The estimate for the uncertainty is achieved as a combination of the upper and lower bounds presented in 3(a), together with an estimate of the statistical error and bias for both.

FIGURE 3. Convergence of the upper and lower bounds for the Bachelier model described in Section 3.5.1 and the resulting relative errors for the American and at-the-money put options.

50-dimensional Bachelier model in Section 3.5.1. Having verified that our numerical implementation reproduces the results expected based on Lemma 2.7, we proceed to apply the method in multivariate Black-Scholes model in Sections 3.5.2-3.5.4.

3.5.1. *American put on a basket in the Bachelier model.* Here we wish to verify the numerical implementation of the finite difference solver for the approximate value function $\overline{\overline{u}}_A$ of (44) and the resulting Monte Carlo estimators, (51) and (50), for the upper and lower bounds, respectively. We examine the solution of a 50-dimensional American put option in the Bachelier model (see equations (2) and (3)). As our prime test case, we focus on the at-the-money put with maturity $T = \frac{1}{4}$. To guarantee a non-trivial early exercise region, we set a relatively high interest rate of $r = 0.05$. We choose an upper diagonal Σ with the diagonal elements $\Sigma_{ii} = 20$ for all assets $1 \le i \le 50$ and draw the off-diagonal components Σ_{ij}, $j > i$ from a standard normal distribution.

Simulating the asset dynamics, $\overline{\overline{X}}$, for a sequence of time discretizations, $N_t = 1000 \times 2^k$, $4 \le k \le 11$, we observe that as N_t increases, the difference between our upper and lower bounds for $u_A(0, \boldsymbol{x})$ becomes negligible. Figure 3(a) shows this behavior of converging bounds, alongside the statistical error of the upper bound estimator, A^+, which is far overshadowed by the corresponding statistical error from the lower bound estimator, A^-. Indeed, as the number of time steps in the forward simulation increases, we see the upper bound intersecting the confidence interval of the lower bound, resulting in the sub-one-percent relative error of the method.

3.5.2. *3-to-1 dimensional Black-Scholes model.* As the first test parametrization of the Black-Scholes model we consider the case of a correlated 3-dimensional Black-Scholes model (see equations(2) and (4)). We decompose the volatility function into the individual volatilities, σ, and the correlation structure of asset returns. We denote with $\mathbf{G}$ the Cholesky decomposition of the correlation matrix of the log-returns

$$(55) \qquad \qquad \Sigma_{ij} = \sigma_i G_{ij}.$$

We set the numerical parameters of our test case to

$$r = 0.05,$$

$$\sigma = (0.2,\ 0.15,\ 0.1)^{\mathrm{T}},$$

$$(56) \qquad \mathbf{G}\mathbf{G}^{\mathrm{T}} = \begin{pmatrix} 1 & 0.8 & 0.3 \\ 0.8 & 1 & 0.1 \\ 0.3 & 0.1 & 1 \end{pmatrix},$$

and a portfolio of equally weighted assets

$$(57) \qquad \qquad \mathbf{P}_1 = [1, 1, 1],$$

as a representative test case of three moderately correlated assets in a high short rate environment. The projected local volatility features noticeable skew, as shown in Figures 1(b) and 2(b).

We evaluate the Laplace-approximated projected volatility, $\tilde{b}$, on a mesh of a few dozen nodes in the region where the the density of the portfolio differs significantly from zero. Performing a regression to a third-degree polynomial on this mesh provides a close fit as seen in Figure 1(a). The third-order approximation also allows us to extend the evaluation of the projected volatility outside the domain in which the Laplace approximation is well behaved. Furthermore, the coefficients of the low-order polynomial fit to the projected volatility are well approximated by a constant, or a linear function of time. This means that for large times we can solve for the projected volatility $\overline{b}^{(x_0)}$ particularly sparsely in time and still have an acceptable interpolation error.

To assess the accuracy of the method, we focus on a set of put options at $T = \frac{1}{2}$ with varying moneyness and report relative numerical accuracy in the approximation of around one percent. For the results of the prices and the corresponding relative errors, we refer to Figure 4.
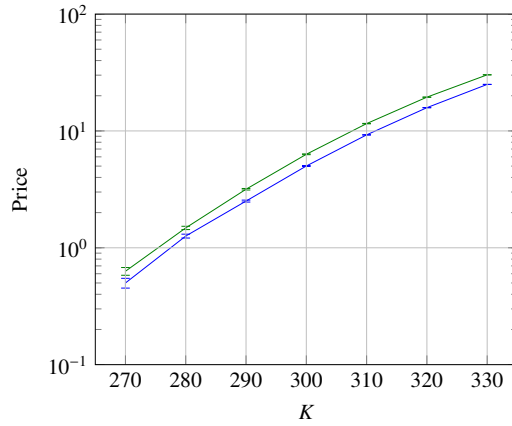
(a) European (Blue) and American (Green) option prices, using forward-Euler Monte Carlo approximation and projected volatility based stopping rule and a martingale bound.
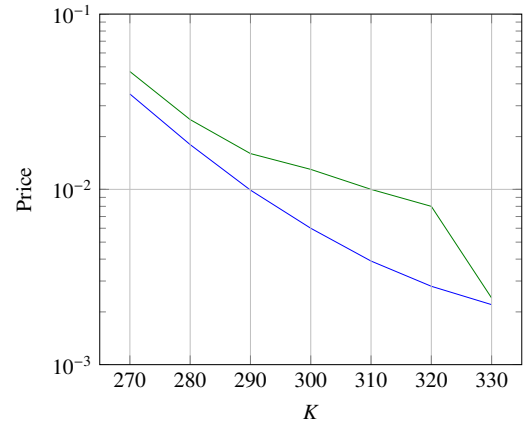
(b) Relative errors in evaluating the American (green) and European (blue) option prices using forward-Euler Monte Carlo approximation for varying ranges of moneyness. At high strike, K we observe trivial stopping time $P\left(\overline{\tau}^{\dagger} = 0\right) = 1$.

FIGURE 4. Both European and American put option prices for the test case (56) and the corresponding relative errors. For comparison of the solvers, identical spatial and temporal meshes, sample sizes and number of Monte Carlo realizations are used for solving both the European and the American options.
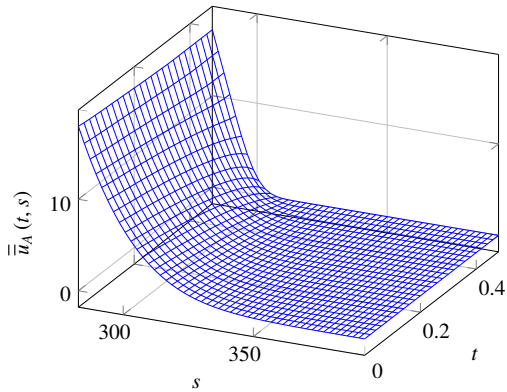
(a) Finite-difference approximation to the American value function of the 3-to-1-dimensional projected problem (56). Note that the values of the value function are used to determine an early-exercise boundary only and have no real-world interpretation except at the point $s = 300$, $t = 0$.
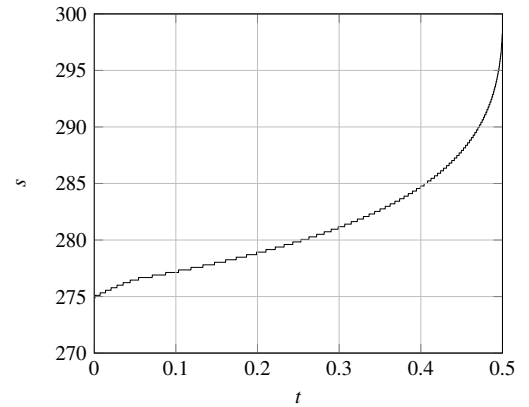
(b) Numerical finite-difference approximation of early exercise boundary of the 3-to-1-dimensional projected problem (56) with maturity $T = 0.5$ for at-the-money put option. A slight kink at $t < 0.05$ resulting from the drop in projected volatility as seen in Figure 1 clearly visible.

FIGURE 5. The value function of the 3-to-1-dimensional Black-Scholes example (56) and the corresponding early exercise boundary.
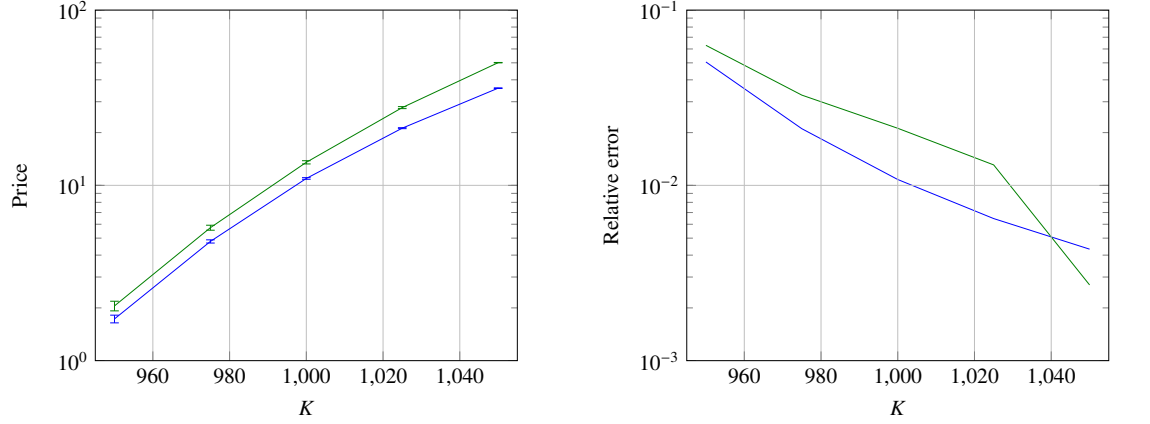
(a) European (Blue) and American (Green) put option prices for the 10-dimensional Black-Scholes test case (58) at $T = 0.5$, using forward-Euler Monte Carlo approximation and projected volatility based stopping rule and a martingale bound.
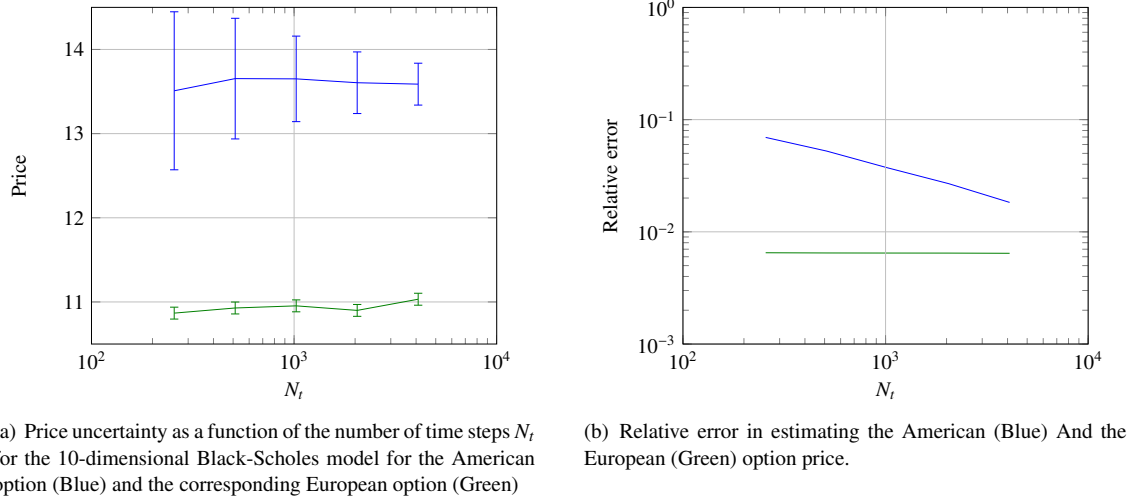
(b) Relative errors in evaluating the American (green) and European (blue) option prices for the 10-dimensional Black-Scholes model (58) using forward-Euler Monte Carlo approximation with varying ranges of moneyness.

FIGURE 6. Convergence of the upper and lower bounds for the 10-to-1 dimensional Black-Scholes model (58) and the resulting relative errors. As in Figure 4, same numerical parameters have been used for solving both the European and the American prices for ease of comparison.

3.5.3. *10-to-1 dimensional Black-Scholes model.* Next, we consider an example similar to (56), increasing the number of dimensions to ten. Continuing with the decomposition (55), we set

$$r = 0.05,$$
$$\sigma_i = 0.125, \ 1 \le i \le 10,$$

$$(58) \quad \mathbf{GG}^{\mathrm{T}} = \begin{pmatrix} 1 & 0.2 & 0.2 & 0.35 & 0.2 & 0.25 & 0.2 & 0.2 & 0.3 & 0.2 \\ 0.2 & 1 & 0.2 & 0.2 & 0.2 & 0.125 & 0.45 & 0.2 & 0.2 & 0.45 \\ 0.2 & 0.2 & 1 & 0.2 & 0.2 & 0.2 & 0.2 & 0.2 & 0.45 & 0.2 \\ 0.35 & 0.2 & 0.2 & 1 & 0.2 & 0.2 & 0.2 & 0.2 & 0.425 & 0.2 \\ 0.25 & 0.125 & 0.2 & 0.2 & 1 & 0.2 & 0.2 & 0.5 & 0.35 & 0.2 \\ 0.2 & 0.45 & 0.2 & 0.2 & 0.2 & 1 & 0.2 & 0.2 & 0.2 & 0.2 \\ 0.2 & 0.45 & 0.2 & 0.2 & 0.2 & 0.2 & 1 & 0.2 & 0.2 & 0.2 \\ 0.2 & 0.2 & 0.2 & 0.2 & 0.2 & 0.2 & 0.2 & 1 & 0.2 & -0.1 \\ 0.3 & 0.2 & 0.45 & 0.425 & 0.5 & 0.35 & 0.2 & 0.2 & 1 & 0.2 \\ 0.2 & 0.45 & 0.2 & 0.2 & 0.2 & 0.2 & 0.2 & -0.1 & 0.2 & 1 \end{pmatrix}.$$

We evaluate a sequence of put options with varying moneyness for the equally weighted portfolio of assets namely we set $P_{1i} = 1$, for all indices. As before, we observe a relative accuracy of a few percent, with decreasing relative error as moneyness increases. As in the previous case, with extreme moneyness, we notice the tendency for an exercise at the initial time, resulting in a variance drop of the estimators and subsequently the relative error, as shown in Figure 6. The behavior of the price uncertainty of the American and European options in the 10-dimensional case, as a function of the number of time steps, N_t, is illustrated in Figure 7(b).

(a) Price uncertainty as a function of the number of time steps N_t for the 10-dimensional Black-Scholes model for the American option (Blue) and the corresponding European option (Green)

(b) Relative error in estimating the American (Blue) And the European (Green) option price.

FIGURE 7. Price uncertainty in the 10-dimensional Black-Scholes model (58) with varying numbers of time steps N_t in the forward-Euler monte Carlo.

3.5.4. *25-to-1 dimensional Black-Scholes model.* Finally, we consider a case with a high dimension that is certainly beyond the reach of most PDE solvers. We choose the 25-dimensional GBM considered by Bayer *et al.* (2016). For the remaining parameters, we set

(59)
$$X_i(0) = 100, \ i \in \{1, 2, \dots, 25\}$$
$$r = 0.05,$$

and evaluate the options with equal portfolio weights, $P_{1i} = 1, i \in \{1, 2, \dots, 25\}$.

With the 25-dimensional model, we continue to observe numerical performance of a few percent of relative errors with the projected stopping rule for basket put options of maturity $T = \frac{1}{2}$ as well as a significant early-exercise premium clearly exceeding the accuracy of the method. Results for the option price estimates for the American and European options and the corresponding error bounds are presented in Figures 8(a) and 8(b), respectively. To demonstrate the consistency and robustness of our approach towards the particular choice of parameters, we replicate the runs multiple times with various portfolio weights. The results of these repeated trials are illustrated in Figure 9.

We note that even though we have not proven asymptotic convergence for a general multivariate model, the approximation of the true problem with the one-dimensional stopping rule gives consistently results that are comparable to the bid-ask spread of the most liquid American index options, and well below those of less-liquid regional indices and ETFs tracking them. We also note that the relative accuracy for the American put price is greatest in the crucial region of in-the money, where the violation of the put-call parity is most profound.

4. CONCLUSIONS

In this work, we have demonstrated the practicability of using Markovian Projection in the framework of pricing American options written on a basket. In the implementation
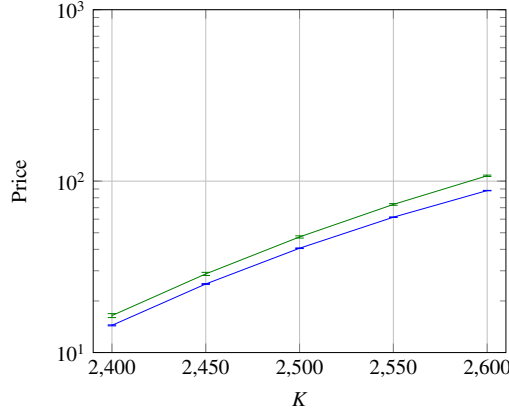
(a) European (Blue) and American (Green) put option prices for the 25-dimensional Black-Scholes test case at $T = 0.5$ of Section 3.5.4, using forward-Euler Monte Carlo approximation and projected volatility based stopping rule and a martingale bound.
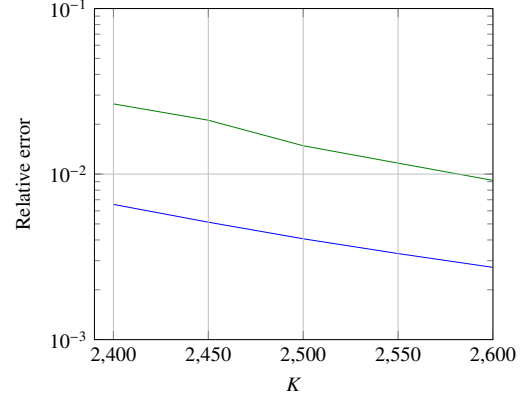
(b) Relative errors in evaluating the American (green) and European (blue) option prices for the 25-dimensional Black-Scholes model using forward-Euler Monte Carlo approximation for varying ranges of moneyness. As in earlier Figures 4 and 6 identical numerical parameters are used for both the American and European options.

FIGURE 8. Convergence of the upper and lower bounds for the 25-to-1-dimensional Black-Scholes model and the resulting relative errors.
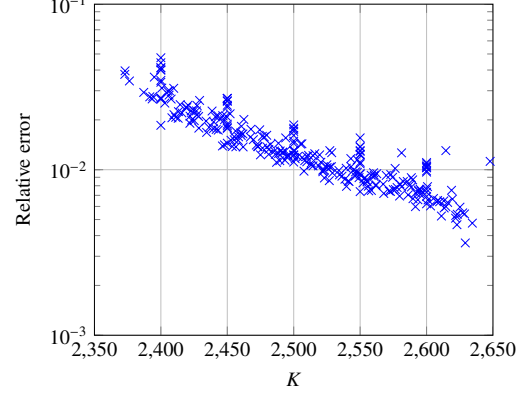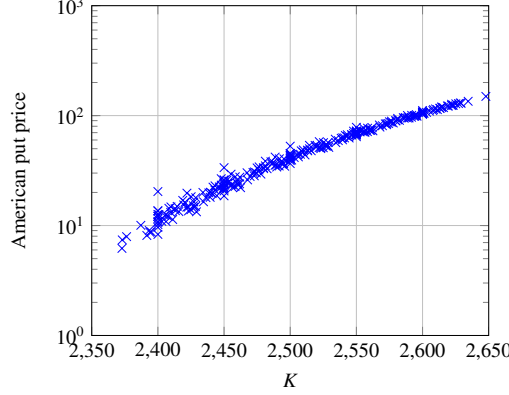

FIGURE 9. American put prices (9(a)) and corresponding relative errors (9(b)) for 43 independent randomized repetitions on evaluating the American put on the 25-to-1-dimensional Black-Scholes model with 258 individual option price valuations for varying strike, K. In addition to the random structure of the test problem by Bayer *et al.* (2016) and the parameters (59) and $T = \frac{1}{4}$, we also randomize the portfolio weights. For each of the runs, we choose P_{1i} independently from an uniform distribution $U[\frac{1}{2}, \frac{3}{2}]$ and finally rescale the weights so that $\sum_{i=1}^{25} P_{1i} = 25$.

of the numerical examples, we have exploited the explicitly known density of the Black-Scholes model, as well as the specific structure of the Bachelier model. Using the known density, we devised a Laplace approximation to evaluate the volatility of a Markovian projection process that describes the projected and approximate dynamics of the basket.

We have shown that for the Bachelier model the Markovian projection gives rise to exact projected option prices, even when considering options with path-dependence. We have also demonstrated how the vanishing derivatives of the cost-to-go function are a manifest of the process dynamics, not the early exercise nature of the option. Leveraging this result, we have demonstrated the existence of nontrivial characterisations of the Black-Scholes model that are essentially of low dimension.

Using the Markovian projection in conjunction with the Laplace approximation, we have implemented low-dimensional approximations of various parametrizations of the multivariate Black-Scholes model. With numerical experiments, we have shown that these approximations perform surprisingly well in evaluating prices of American options written on a basket. We interpret these results as a manifestation of the Black-Scholes model being well approximated by a corresponding Bachelier model. What sets these results apart from many of the earlier works is the fact that we approximate the full trajectory of a basket of assets in the Black-Scholes model, not only instantaneous returns.

The primary method used to solve such problems so far has been the least-squares Monte Carlo method that shares some common attributes with our proposed method. Unlike least-squares Monte Carlo, our proposed method does not rely on a choice of basis vectors that are used to evaluate the holding price of an option, but only on the direction or directions along which we evaluate the projected dynamics.

Our results leave the door open for future developments including the extension of the current research into models beyond the GBM model. We validate the accuracy of our stopping rule using a forward-simulation. One possible extension of this work would be to use the forward sample also to evaluate the projected volatilities, an approach used in calibration of correlation structures by Guyon (2015). As the only non-controlled error in our method is the bias incurred in evaluating the local volatility $\overline{b}^{(x_0)}$, the possibility to implement such an evaluation efficiently but without introducing bias would be very useful. From a theoretical viewpoint, our work raises the question of whether the approximation improves if the projection dimension is increased.

In this work, we have not aimed to demonstrate the use of Markovian-projected models for evaluating implied stopping times. In doing so, we have not aimed for the greatest possible computational efficiency, and many possibilities for further optimization exist in this area. In terms of orders of convergence, the bottleneck of the computation is the forward Euler simulation and subsequent evaluation of maxima and hitting times of realizations of an SDE. These Monte Carlo methods could be enhanced through adaptivity, multi-level methods, use of quasi-Monte Carlo (Birge, 1994; Joy *et al.*, 1996), or analytic approximations. Likewise, there is a possibility for optimization of the numerical solver to evaluate the value function using a highly optimized backward solver (Khaliq *et al.*, 2008). For the possibility of extending the projection to higher dimensions to allow for higher-dimensional approximation of the early exercise boundary, we refer reader to (Hager *et al.*, 2010). We also note the possibility of using a binomial tree method (Joshi, 2007), that naturally takes into account the shape of the domain $\overline{D}$ for the projected PDE.

We have focused on the commercially most relevant application of American options that are widely quoted on the market. For the case of binary options the analysis remains

identical, only the functional form of the payoff g changes. It would also be of interest to study the performance of the Markovian-projected dynamics in pricing other path-dependent options such as Asian and knockoff options. Study of more general payoff functions is possible, assuming the projected volatility corresponding to these state variables could be efficiently evaluated.

References

Achdou, Y. and Pironneau, O., *Computational methods for option pricing*, 2005, SIAM.

Ametrano, F. and Ballabio, L., QuantLib - a free/open-source library for quantitative finance. , 2003.

Bally, V., Printems, J. *et al.*, A quantization tree method for pricing and hedging multidimensional American options. *Mathematical finance*, 2005, **15**, 119–168.

Barraquand, J. and Martineau, D., Numerical valuation of high dimensional multivariate American securities. *Journal of financial and quantitative analysis*, 1995, **30**, 383–405.

Bayer, C. and Laurence, P., Asymptotics beats Monte Carlo: The case of correlated local vol baskets. *Communications on Pure and Applied Mathematics*, 2014, **67**, 1618–1657.

Bayer, C., Siebenmorgen, M. and Tempone, R., Smoothing the payoff for efficient computation of basket option prices. *arXiv preprint arXiv:1607.05572*, 2016.

Bayer, C., Szepessy, A. and Tempone, R., Adaptive weak approximation of reflected and stopped diffusions. *Monte Carlo Methods and Applications*, 2010, **16**, 1–67.

Belomestny, D., Dickmann, F. and Nagapetyan, T., Pricing American options via multilevel approximation methods. *arXiv preprint arXiv:1303.1334*, 2013.

Belomestny, D., Dickmann, F. and Nagapetyan, T., Pricing Bermudan options via multilevel approximation methods. *SIAM Journal on Financial Mathematics*, 2015, **6**, 448–466.

Birge, J.R., Quasi-Monte Carlo approaches to option pricing. *Ann Arbor*, 1994, **1001**, 48109.

Black, F. and Scholes, M., The pricing of options and corporate liabilities. *The journal of political economy*, 1973, pp. 637–654.

Broadie, M. and Glasserman, P., Pricing American-style securities using simulation. *Journal of Economic Dynamics and Control*, 1997, **21**, 1323–1352.

Buchmann, F., Computing exit times with the Euler scheme. In *Proceedings of the Seminar für Angewandte Mathematik, Eidgenössische Technische Hochschule*, 2003.

Choi, S. and Marcozzi, M.D., A numerical approach to American currency option valuation. *The Journal of Derivatives*, 2001, **9**, 19–29.

Cont, R., Empirical properties of asset returns: stylized facts and statistical issues. , 2001.

Cox, J., Notes on option pricing I: Constant elasticity of variance diffusions. *Unpublished note, Stanford University, Graduate School of Business*, 1975.

Djehiche, B. and Löfdahl, B., Risk aggregation and stochastic claims reserving in disability insurance. *Insurance: Mathematics and Economics*, 2014, **59**, 100–108.

Fama, E.F., The behavior of stock-market prices. *The journal of Business*, 1965, **38**, 34–105.

Feng, L., Kovalov, P., Linetsky, V. and Marcozzi, M., Variational methods in derivatives pricing. *Handbooks in Operations Research and Management Science*, 2007, **15**, 301–342.

Giles, M.B., Multilevel Monte Carlo methods. *Acta Numerica*, 2015, **24**, 259.

Glasserman, P., Yu, B. *et al.*, Number of paths versus number of basis functions in American option pricing. *The Annals of Applied Probability*, 2004, **14**, 2090–2119.

Goutis, C. and Casella, G., Explaining the saddlepoint approximation. *The American Statistician*, 1999, **53**, 216–224.

Grunspan, C., A Note on the Equivalence between the Normal and the Lognormal Implied Volatility: A Model Free Approach. *Available at SSRN 1894652*, 2011.

Guyon, J., Cross-dependent volatility. *Available at SSRN 2615162*, 2015.

Gyöngy, I., Mimicking the one-dimensional marginal distributions of processes having an Itô differential. *Probability theory and related fields*, 1986, **71**, 501–516.

Hager, C., Hüeber, S. and Wohlmuth, B.I., Numerical techniques for the valuation of basket options and their Greeks. *The Journal of Computational Finance*, 2010, **13**, 3.

Haugh, M.B. and Kogan, L., Pricing American options: a duality approach. *Operations Research*, 2004, **52**, 258–270.

Hilber, N., Matache, A.M. and Schwab, C., Sparse wavelet methods for option pricing under stochastic volatility. In *Proceedings of the* , 2004.

Joshi, M.S., The convergence of binomial trees for pricing the American put. *Available at SSRN 1030143*, 2007.

Joy, C., Boyle, P.P. and Tan, K.S., Quasi-Monte Carlo methods in numerical finance. *Management Science*, 1996, **42**, 926–938.

Kangro, R. and Nicolaides, R., Far Field Boundary Conditions for Black–Scholes Equations. *SIAM Journal on Numerical Analysis*, 2000, **38**, 1357–1368.

Khaliq, A.Q., Voss, D.A. and Kazmi, K., Adaptive θ-methods for pricing American options. *Journal of Computational and Applied Mathematics*, 2008, **222**, 210–227.

Longstaff, F.A. and Schwartz, E.S., Valuing American options by simulation: a simple least-squares approach. *Review of Financial studies*, 2001, **14**, 113–147.

Mandelbrot, B.B., The variation of certain speculative prices. In *Fractals and Scaling in Finance*, pp. 371–418, 1997, Springer.

Matache, A.M., Von Petersdorff, T. and Schwab, C., Fast deterministic pricing of options on Lévy driven assets. *ESAIM: Mathematical Modelling and Numerical Analysis*, 2004, **38**, 37–71.

Mehta, N.B., Wu, J., Molisch, A.F. and Zhang, J., Approximating a sum of random variables with a lognormal. *IEEE Transactions on Wireless Communications*, 2007, **6**.

Melino, A. and Turnbull, S.M., The pricing of foreign currency options. *Canadian Journal of Economics*, 1991, pp. 251–281.

Merton, R.C., Brennan, M.J. and Schwartz, E.S., The valuation of American put options. *The Journal of Finance*, 1977, **32**, 449–462.

Piterbarg, V., A stochastic volatility forward Libor model with a term structure of volatility smiles. *SSRN eLibrary*, 2003.

Piterbarg, V., Markovian projection method for volatility calibration. *Available at SSRN 906473*, 2006.

Piterbarg, V.V., Stochastic Volatility Model with Time-dependent Skew. *Applied Mathematical Finance*, 2005, **12**, 147–185.

Rogers, L.C., Monte Carlo valuation of American options. *Mathematical Finance*, 2002, **12**, 271–286.

Schachermayer, W. and Teichmann, J., How close are the option pricing formulas of Bachelier and Black–Merton–Scholes?. *Mathematical Finance*, 2008, **18**, 155–170.

Shun, Z. and McCullagh, P., Laplace approximation of high dimensional integrals. *Journal of the Royal Statistical Society. Series B (Methodological)*, 1995, pp. 749–760.

Sullivan, E.J. and Weithers, T.M., Louis Bachelier: The father of modern option pricing theory. *The Journal of Economic Education*, 1991, **22**, 165–171.

Thomson, I.A., Option Pricing Model: Comparing Louis Bachelier with Black-Scholes Merton. *Available at SSRN*, 2016.

Yosida, K., On the fundamental solution of the parabolic equation in a Riemannian space. *Osaka Mathematical Journal*, 1953, **5**, 65–74.

Zanger, D.Z., Quantitative error estimates for a least-squares Monte Carlo algorithm for American option pricing. *Finance and Stochastics*, 2013, **17**, 503–534.

Zanger, D.Z., Convergence of a least-squares Monte Carlo algorithm for American option pricing with dependent sample data. *Mathematical Finance*, 2016.

Appendix A. Laplace approximation

The Taylor expansion of the integrands in equation (39) can be done in various ways, and we discuss and illustrate some natural choices here. For the test case, let us consider the equal-volatility, equal weight non-correlated two-dimensional Black-Scholes model with $r = 0$ and

$$\mathbf{P}_1 = [1, 1],$$
$$\mathbf{\Sigma} = \text{diag}\left([\sigma, \sigma]^{\mathrm{T}}\right),$$
$$\mathbf{X}(0) = [100, 100]^{\mathrm{T}},$$

with the volatility, $\sigma = 0.1$. For such a simple test case, we can evaluate the relevant expansion by hand. For a high-dimensional model, we need to resort to quadratures or Monte Carlo.

Fixing the portfolio value to $\mathbf{P}_1\mathbf{X}(0)$, the relevant unimodal integrands in terms of the natural price of the second asset s_2 are given as

(60)
$$f_1(s_2) = \frac{\exp\left(-\frac{\left(\log\left(2-\frac{s_2}{100}\right)\right)^2}{2\sigma^2} - \frac{\left(\log\frac{s_2}{100}\right)^2}{2\sigma^2} + 2\log\sigma + \log\left(s_2^2 - 400s^2 + 40000\right) - \log\left(200 - s_2\right) - \log s_2\right)}{2\pi\sigma^2}$$

for the numerator and

(61)
$$\tilde{f}_1(s_2) \frac{\exp\left(-\frac{\left(\log\left(2-\frac{s_2}{100}\right)\right)^2}{2\sigma^2} - \frac{\left(\log\frac{s_2}{100}\right)^2}{2\sigma^2} - \log\left(200 - s_2\right) - \log s_2\right)}{2\pi\sigma^2}$$

for the denominator. Alternatively, we can express the integrals in terms of log-price $x_2 = \log\frac{s_2}{100}$,

(62)
$$f_2(x_2) = \frac{-\frac{\left(\log(2-e^{x_2})\right)^2}{2\sigma^2} - \frac{x_2^2}{2\sigma^2} + 2\log\sigma + \log\left(2e^{2x_2} - 4e^{x_2} + 4\right) - \log\left(2 - e^{x_2}\right) - x_2}{2\pi\sigma^2}$$

for the numerator and

(63)
$$\tilde{f}_2(x_2) = \frac{-\frac{\left(\log(2-e^{x_2})\right)^2}{2\sigma^2} - \frac{x_2^2}{2\sigma^2} - \log\left(2 - e^{x_2}\right) - x_2}{2\pi\sigma^2}$$
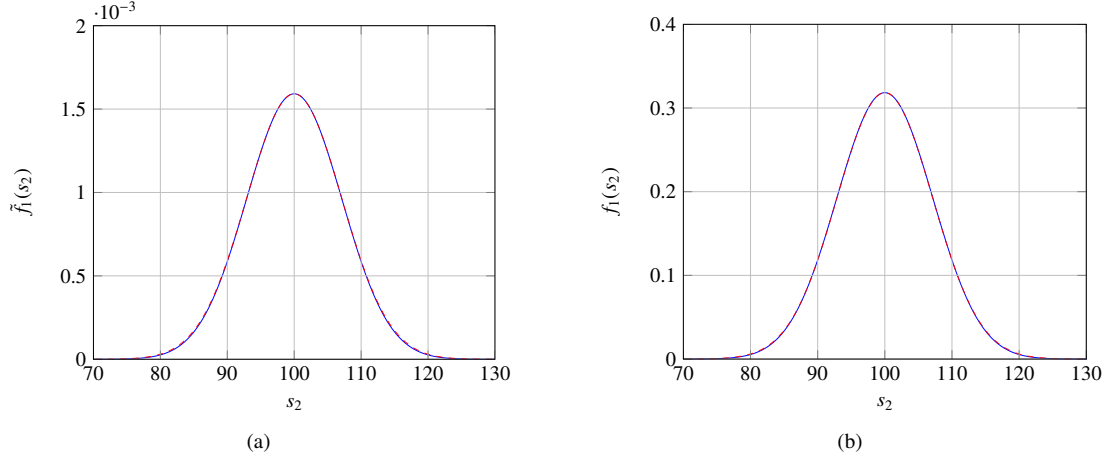
(a)   (b)

FIGURE 10. Functions f_1 of (61) (10(a)) and $\tilde{f}_1$ of (60) (10(b)) in blue and their respective approximations based on the second-order Taylor expansions of their logarithms in dashed red.
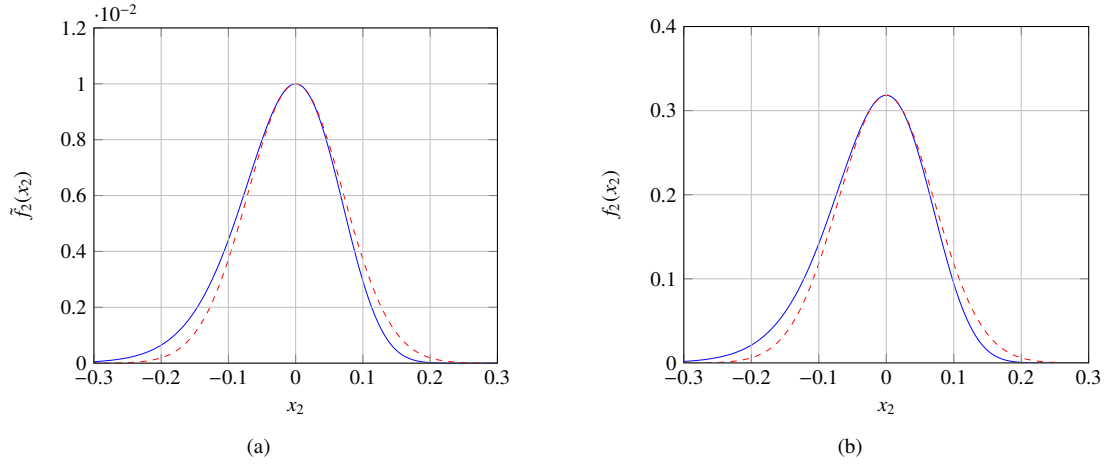

(a)   (b)

FIGURE 11. Functions f_2 of (63) (11(a)) and $\tilde{f}_2$ of (62) (11(b)) in blue and and their respective approximations based on the second-order Taylor expansions of their logarithms in dashed red.

for the denominator. With these definitions we have the unit-time projected volatility

$$\left(\bar{b}^{(x_0)}\right)^2 (1, 200) = \frac{\int_{\mathbb{R}} f_1(s_2)\,\mathrm{d}s_2}{\int_{\mathbb{R}} \tilde{f}_1(s_2)\,\mathrm{d}s_2} = \frac{\int_{\mathbb{R}} f_2(x_2)\,\mathrm{d}x_2}{\int_{\mathbb{R}} \tilde{f}_2(x_2)\,\mathrm{d}x_2}.$$

The integrands f_1, $\tilde{f}_1$ and their respective second-order approximations of the form $\exp\left(\eta + \kappa(z_2 - z^*)^2\right)$ are illustrated in Figure 10 for the price expansion and in Figure 11, log-price respectively.

The approximations are given as

$$2\pi\sigma^2 f_1(s_2) \approx \exp\left(2\log\sigma - \left(\frac{1}{100^2\sigma^2} + \frac{2}{100^2}\right)(s_2 - 100)^2\right),$$

$$2\pi\sigma^2 \tilde{f}_1(s_2) \approx \exp\left(-2\log 200 - \left(\frac{1}{100^2\sigma^2} + \frac{1}{100^2}\right)(s_2 - 100)^2\right),$$

$$2\pi\sigma^2 f_2(x_2) \approx \exp\left(2\log\sigma + \log 200 - \left(\frac{1}{\sigma^2} + 2\right)x_2^2\right),$$

$$2\pi\sigma^2 \tilde{f}_2(x_2) \approx \exp\left(-\left(\frac{1}{\sigma^2} + 1\right)x_2^2\right),$$

giving for both approximations

$$\tilde{b}_1^2(1, 100) = \tilde{b}_2^2(1, 100) = 20000\sigma^2 \sqrt{\frac{1 + 2\sigma^2}{1 + \sigma^2}} \approx 200.99.$$

In contrast, with quadrature, we get a reference value of 200.98, giving a close agreement with the Laplace-approximated value.

Weierstrass Institute, Mohrenstrasse 39, 10117 Berlin, Germany
E-mail address: christian.bayer@wias-berlin.de

CEMSE, King Abdullah University of Science and Technology (KAUST), Thuwal 23955-6900, Saudi Arabia
E-mail address: juho.happola@kaust.edu.sa

CEMSE, King Abdullah University of Science and Technology (KAUST), Thuwal 23955-6900, Saudi Arabia
E-mail address: raul.tempone@kaust.edu.sa